JEM Journal of Experimental Medicine

ARTICLE

Thyrotropin aggravates atherosclerosis by promoting macrophage inflammation in plaques

Chongbo Yang[1*], Ming Lu[1*], Wenbin Chen[2], Zhao He[1,4], Xu Hou[1], Mei Feng[2], Hongjia Zhang[3], Tao Bo[2], Xiaoming Zhou[2], Yong Yu[5], Haiqing Zhang[1], Meng Zhao[1], Laicheng Wang[2], Chunxiao Yu[1], Ling Gao[2], Wenjian Jiang[3], Qunye Zhang[6], and Jiajun Zhao[1]

Subclinical hypothyroidism is associated with cardiovascular diseases, yet the underlying mechanism remains largely unknown. Herein, in a common population (*n* = 1,103), TSH level was found to be independently correlated with both carotid plaque prevalence and intima-media thickness. Consistently, TSH receptor ablation in *ApoE*$^{-/-}$ mice attenuated atherogenesis, accompanied by decreased vascular inflammation and macrophage burden in atherosclerotic plaques. These results were also observed in myeloid-specific *Tshr*-deficient *ApoE*$^{-/-}$ mice, which indicated macrophages to be a critical target of the proinflammatory and atherogenic effects of TSH. In vitro experiments further revealed that TSH activated MAPKs (ERK1/2, p38α, and JNK) and IκB/p65 pathways in macrophages and increased inflammatory cytokine production and their recruitment of monocytes. Thus, the present study has elucidated the new mechanisms by which TSH, as an independent risk factor of atherosclerosis, aggravates vascular inflammation and contributes to atherogenesis.

Introduction

Hypothyroidism has been well recognized to be accompanied by hypercholesterolemia and cardiovascular diseases (Jones et al., 1955). Traditionally, this is attributed to the decreased thyroid hormone levels in these patients (Cappola and Ladenson, 2003; Collet et al., 2014; Delitala et al., 2017). However, increased risk of hypercholesterolemia and cardiovascular diseases including atherosclerosis are also found among subclinical hypothyroidism (SH) patients, whose thyroid hormone levels remain normal and only thyroid-stimulating hormone (TSH) levels are increased (Hak et al., 2000; Rodondi et al., 2010; Collet et al., 2014). This suggests that TSH may also play roles in atherosclerosis independent from its influence on thyroid hormones.

TSH, also named thyrotropin, is a glycoprotein hormone synthesized and secreted by the pituitary, well known for its classic role in the hypothalamus–pituitary–thyroid axis to stimulate thyroid hormone synthesis and secretion from thyroid gland (Marians et al., 2002). Mere decades ago, TSH receptors (TSHR) were discovered to be expressed in a variety of cells apart from thyrocytes, such as hepatocytes (Tian et al., 2010), adipocytes (Ma et al., 2015), and osteoclasts (Abe et al., 2003). This indicates that the function of TSH is not confined to the regulation of thyroid function. Previously, it was shown that TSH indeed could bind to the TSHR on hepatocytes and modulate liver cholesterol synthesis and transformation, thereby directly contributing to hypercholesterolemia (Tian et al., 2010; Song et al., 2015). However, apart from its effect on cholesterol, it still remains unknown whether TSH can contribute to atherosclerosis in other ways, e.g., by directly promoting the vascular inflammation that is central to all stages of atherosclerosis. On the other hand, TSHR has also been reported to be expressed in macrophages, endothelial cells, and smooth muscle cells (Sellitti et al., 2000; Klein, 2003; Lu et al., 2015). These three types of cells are most critically involved in atherosclerosis. Therefore, it is very possible that TSH can promote atherosclerosis not only indirectly by regulating thyroid function, but also directly by acting on these cells.

To test the above hypothesis, the association between TSH and atherosclerosis was first analyzed in a cross-sectional population study. The grade of atherosclerosis in the population was monitored by carotid intima-media thickness (CIMT)

[1]Department of Endocrinology, Shandong Provincial Hospital affiliated to Shandong University, Shandong Key Laboratory of Endocrinology and Lipid Metabolism, Institute of Endocrinology and Metabolism, Shandong Academy of Clinical Medicine, Jinan, Shandong, China; [2]Scientific Center, Shandong Provincial Hospital affiliated to Shandong University, Jinan, Shandong, China; [3]Department of Cardiac Surgery, Beijing Anzhen Hospital, Capital Medical University, Beijing Institute of Heart, Lung and Blood Vessel Diseases, Beijing Laboratory for Cardiovascular Precision Medicine, Beijing, China; [4]School of Medicine, Shandong University, Jinan, Shandong, China; [5]Department of Sonography, Shandong Provincial Hospital affiliated to Shandong University, Jinan, Shandong, China; [6]Key Laboratory of Cardiovascular Remodeling and Function Research, Chinese Ministry of Education and Ministry of Public Health, the State and Shandong Province Joint Key Laboratory of Translational Cardiovascular Medicine, Qilu Hospital of Shandong University, Jinan, Shandong, China.

*C. Yang and M. Lu contributed equally to this paper; Correspondence to Jiajun Zhao: jjzhao@sdu.edu.cn; Qunye Zhang: wz.zhangqy@sdu.edu.cn.

measurement by ultrasonography, a simple, noninvasive method that is well suited for evaluating atherosclerosis in large-scale population studies (Lorenz et al., 2007; Bis et al., 2011). The causal relationship between TSH and atherosclerosis was then demonstrated using *Tshr*$^{-/-}$ *ApoE*$^{-/-}$ double knockout mice. Moreover, in vitro study revealed a novel proinflammatory effect of TSH on the macrophages, and its pathophysiological significance was further confirmed using myeloid-specific *Tshr*-deficient *ApoE*$^{-/-}$ mice. Thereby, our study provides mechanistic insights into the predisposition to atherosclerosis in overt hypothyroidism and SH and comes up with a previously unrecognized proinflammatory and atherogenic role of TSH.

Results

TSH positively correlates with inflammation and atherosclerosis in the population

To explore the relationship between TSH and atherosclerosis, a cross-sectional population study enrolling 2,480 volunteers was performed. After excluding subjects with conditions that can affect atherosclerosis, thyroid function, and/or abnormal free thyroxine (FT4) levels, the remaining subjects (n = 1,103) were divided into three groups (euthyroid controls, mild SH, and severe SH) based on their TSH levels (Fig. 1 A; Cooper and Biondi, 2012). Basic clinical characteristics of the participants are summarized in Table 1. Serum total cholesterol (TC) and low-density lipoprotein cholesterol (LDL-C) levels in mild and severe SH were significantly elevated compared with euthyroid controls ($P < 0.01$). Serum triglyceride (TG) and high-density lipoprotein cholesterol (HDL-C) levels were similar between SH and euthyroid populations. There was no significant difference in FT3, body mass index, diastolic blood pressure, or fasting plasma glucose (FPG) levels among these groups. Rates of smoking and drinking were also similar among the three groups.

The populations with higher TSH levels showed significant increased prevalence of carotid plaque (Fig. 1 B) and CIMT (Fig. 1 C). Moreover, the positive correlation between TSH and CIMT remained significant even when traditional cardiovascular factors including age, dyslipidemia, and blood pressure, were controlled by multiple linear regression analysis (Table 2), which continued to be true when only male or female subjects were analyzed (data not shown). Moreover, serum levels of several critical inflammatory factors including TNF-α, CCL-2, and IL-1β were also significantly increased in the SH population (Fig. 1, D–H). These findings support an association between TSH and atherosclerosis that is independent from traditional cardiovascular factors and thyroid function and is related to inflammation in the population.

Global *Tshr* knockout attenuates atherogenesis and vascular inflammation

The above findings implied a direct effect of TSH on atherosclerosis independent of other traditional risk factors and its classic roles, which is further supported by the presence of TSH in atherosclerotic lesions (Fig. S1, A and B). To examine the causal relationship of TSH and atherogenesis, *Tshr*$^{-/-}$*ApoE*$^{-/-}$ and *Tshr*$^{+/+}$*ApoE*$^{-/-}$ littermates were obtained by crossing *Tshr*$^{+/-}$ mice with *ApoE*$^{-/-}$ mice. Mice were fed a Western diet (WD) beginning at 6 wk of age and sacrificed 12 or 16 wk afterwards. *Tshr*$^{-/-}$*ApoE*$^{-/-}$ mice were maintained euthyroid by thyroxine powder supplementation in the diet after weaning to exclude the interference of abnormal thyroid hormone levels (Fig. 2 A; Marians et al., 2002). The body weights (Fig. S1 C) and serum T3, T4, and TSH levels (Fig. S1, D–F) were comparable between *Tshr*$^{-/-}$*ApoE*$^{-/-}$ mice and *Tshr*$^{+/+}$*ApoE*$^{-/-}$ mice, meaning the dose of the supplemented thyroxine was appropriate. These results ruled out the possibility that thyroid hormones had interfered with the endpoints of *Tshr*$^{-/-}$*ApoE*$^{-/-}$.

Lipid parameters were comparable between two groups (Fig. S1, G–J). However, Oil Red O staining of the aorta and aortic root revealed a significant reduction in plaque area in *Tshr*$^{-/-}$*ApoE*$^{-/-}$ mice (Fig. 2, B and C), accompanied by reduced signs of lesion progression (Fig. S1, K and L). F4/80^{+} area (Fig. 2 D) and MOMA-2^{+} area (Fig. S1 M) in the plaques were significantly reduced in *Tshr*$^{-/-}$*ApoE*$^{-/-}$ mice, suggesting relieved macrophage burden. *Tshr*$^{-/-}$*ApoE*$^{-/-}$ mice also showed attenuated vascular inflammation, with reduced expression of *F4/80*, *Il-1b*, *Il-6*, *Tnfa*, and *Ccl2* (Fig. 2 E) in the aorta. The result was confirmed by immunohistochemistry (IHC) of TNF-α and IL-6 (Fig. 2, F and G). Serum levels of IL-6 and TNF-α were also significantly decreased in *Tshr*$^{-/-}$*ApoE*$^{-/-}$ mice (Fig. 2, H and I). On the contrary, neither smooth muscle cells nor collagen content was significantly altered by *Tshr* knockout (Fig. S1, N and O). The above results suggest that TSH can promote vascular inflammation and atherosclerosis by certain thyroid hormone–independent mechanisms.

TSH promotes macrophage inflammation directly

Because macrophages play a pivotal role in atherosclerosis, and also are remarkably affected by *Tshr* ablation (Fig. 2 D and Fig. S1 M), we wondered whether macrophages were directly affected by TSH. TSHR expression in mouse peritoneal macrophages (Fig. 3 A) and plaque macrophages (Fig. S2 A) was first confirmed by immunofluorescence. Macrophages were then treated with TSH in vitro, and a dose-dependent induction of TNF-α and IL-6 was observed (Fig. 3, B and C). Moreover, TSH significantly up-regulated *Nos2*, *Il6*, and *Tnfa*, three markers implicated in acute inflammation, and down-regulated a series of markers related to inflammation resolution, including *Arg1*, *Pparg*, *Lxra*, and *Abca1* (Fig. 3 D) in the presence of Ox-LDL. Therefore, TSH does promote macrophage inflammation directly.

Notably, *Ccl2* and *Cx3cl1*, two chemokines previously reported to be critical for monocyte recruitment in atherosclerosis (Gosling et al., 1999; Saederup et al., 2008; Drechsler et al., 2015), were also found to be greatly induced by TSH incubation in macrophages (Fig. 3 D). We then examined the effect of TSH on monocyte recruitment by a Transwell assay in vitro. In this setting, bone marrow–derived macrophages (BMDMs) in conditioned medium were placed in the lower chamber to attract the murine bone marrow monocytes added to the upper chamber (Fig. S2 B). The purity of the monocytes was verified by flow cytometry (FCM; Fig. S2 C). TSH treatment rendered the macrophage conditioned medium much more attractive to monocytes (Fig. 3 E), and the ablation of the *Tshr* of the macrophages efficiently reversed this phenomenon (Fig. 3 E). Consistently,

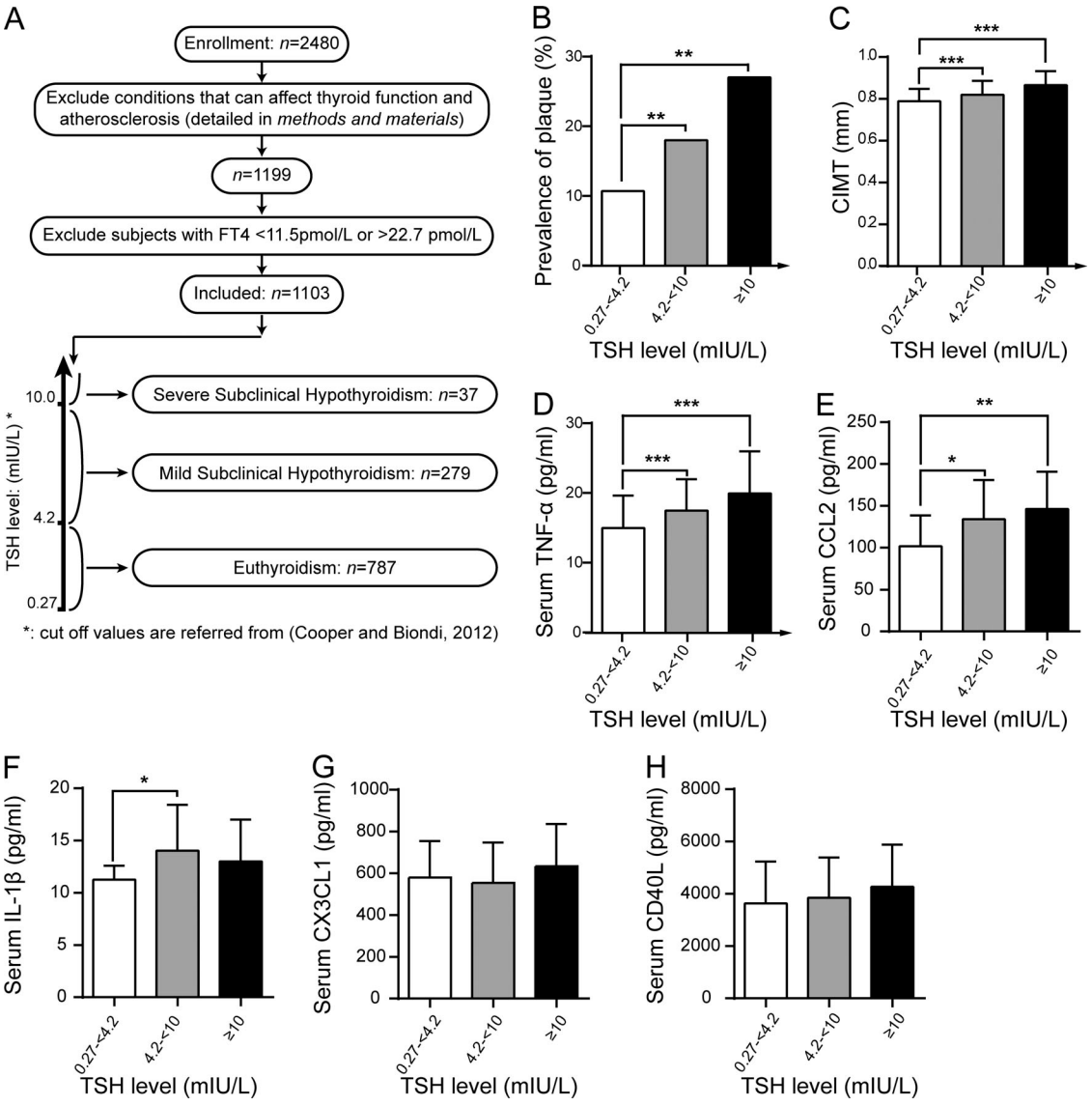

Figure 1. **TSH correlated positively with both atherosclerosis and inflammation in the population. (A)** After exclusion criteria were applied, the included subjects were divided into three groups: euthyroidism (0.27 ≤ TSH < 4.2), mild SH (4.2 ≤ TSH < 10), and severe SH (10 ≤ TSH). **(B and C)** The prevalence of carotid plaque (B) and CIMT (C) detected by ultrasonography in populations with different serum TSH levels. Sample size (*n*) is indicated in A. **(D–H)** Serum TNF-α (D) detected by ELISA and CCL2 (E), IL-1β (F), CX3CL1 (G), and CD40L (H) levels in each group. Subjects were selected randomly from the included population (*n* = 24 for each group). The data represent the mean ± SD. Difference in prevalence was compared with crosstab χ^2 or Fisher's exact test when appropriate. In other cases, the differences were compared with one-way ANOVA and post hoc Dunnett *t* test using euthyroid group as control. *, P < 0.05; **, P < 0.01; ***, P < 0.001.

adding TSH alone in the lower chamber showed no chemotactic effect on monocytes (Fig. S2 D).

Besides monocyte recruitment, macrophage burden in the plaque is also related to factors such as the maturation, apoptosis, and proliferation of macrophages. TSH does not accelerate monocyte maturation, as no difference was found between the differentiation of *Tshr*$^{-/-}$ and *Tshr*$^{+/+}$ BMDMs (Fig. S2, E–H). Consistently, TSH also showed no significant effect on the expression of F4/80 expression of monocytes (Fig. 3 F) or the apoptosis of macrophages in the presence of oxidized LDL (OxLDL; Fig. 3 G). Therefore, *Tshr* knockout might not relieve macrophage burden by decreasing the differentiation of monocytes into macrophages or increasing the apoptosis of macrophage.

Myeloid-specific *Tshr* knockout suppresses vascular inflammation and delayed atherosclerosis

To test the in vivo relevance of the proinflammatory effect of TSH on macrophages in vascular inflammation and atherogenesis, we generated myeloid-specific *Tshr* knockout mice with *ApoE*$^{-/-}$ background (genotype: *LyzM-Cre*$^{+}$ *Tshr*$^{flox/flox}$ *ApoE*$^{-/-}$, denoted as TSHR^{MKO} hereafter) by crossing *Tshr*$^{flox/flox}$ (Fig. S3 A), *LyzM-Cre*$^{+}$, and *ApoE*$^{-/-}$ mice. Freshly isolated bone marrow cells (D0) from TSHR^{MKO} mice showed an insignificant decrease in *Tshr* transcription compared with those of their littermate controls (LC; Fig. S3 B). However, the gap in *Tshr* transcription levels between the two genotypes widened remarkably after 7 d of differentiation toward BMDMs (Fig. S3 B), meaning the

Table 1. **The characteristics of included subjects stratified according to serum TSH concentration**

Characteristic	Total	Euthyroid	Mild SH	Severe SH	P value
Serum TSH (mIU/liter)		0.27 ≤ TSH < 4.2	4.2 ≤ TSH < 10	10 ≤ TSH	
Age (yr)	54.32 (7.65)	53.59 (7.28)	55.81 (8.24)[a]	58.84 (8.14)[a,b]	**<0.001**
Male sex	291 (26.3)	244 (31.0)	42 (15.1)	5 (13.5)	**<0.001**
Smoking	482 (43.7)	338 (42.9)	126 (45.2)	18 (48.6)	0.673
Drinking	305 (27.6)	230 (29.2)	28 (24.4)	7 (18.9)	0.079
BMI (kg/m^2)	25.22 (3.53)	25.13 (3.56)	25.34 (3.46)	26.15 (3.24)	0.276
SBP (mm Hg)	134.04 (18.79)	131.63 (18.36)	139.84 (18.71)[a]	142.08 (18.18)[a]	**<0.001**
DBP (mm Hg)	79.92 (11.49)	79.40 (11.92)	81.39 (10.10)[a]	80.16 (11.74)	0.075
FT3 (pmol/ml)	4.91 (0.64)	4.93 (0.66)	4.90 (0.60)	4.83 (0.55)	0.702
FT4 (pmol/ml)	15.69 (2.17)	16.24 (2.05)	14.45 (1.85)[a]	13.50 (1.57)[a,b]	**<0.001**
TSH (mIU/liter)	2.96 (2.58)	2.32 (1.49)	5.45 (2.12)	11.63 (2.72)	N/A
TC (mmol/liter)	5.19 (1.19)	5.01 (1.15)	5.63 (1.16)[a]	5.86 (1.28)[a]	**<0.001**
TG (mmol/liter)	1.10 (0.75)	1.04 (0.73)	1.22 (0.82)	1.32 (0.73)	0.363
LDL-C (mmol/liter)	3.00 (0.86)	2.91 (0.84)	3.20 (0.83)[a]	3.47 (0.95)[a,b]	**<0.001**
HDL-C (mmol/liter)	1.42 (0.33)	1.41 (0.33)	1.46 (0.35)[a]	1.40 (0.30)	0.141
FPG (mmol/liter)	5.78 (0.99)	5.78 (1.01)	5.79 (0.94)	5.57 (0.84)	0.537

Intergroup comparisons were done with post-hoc Hochberg's GT2 test. Data are expressed as the mean (SD) or median (interquantile range) depending on the type of variance. TG was log-transformed before being analyzed by one-way ANOVA. Bold text indicates that P values are statistically significant. BMI, body mass index; DBP, diastolic blood pressure; SBP, systolic blood pressure.
[a]P < 0.05 vs. euthyroid control.
[b]P < 0.05 vs. mild SH.

knockout is specific. The efficiency of the knockout was estimated to be >95% by day 7 (Fig. S3 B).

Then, TSHR^{MKO} mice and their littermates were fed a WD for 12 or 16 wk. Similar to global knockout mice, TSHR^{MKO} mice had similar body weight, thyroid function, and serum lipid profile compared with their littermates (Fig. S3, C–J); however, the levels of serum IL-6 and CCL2 in TSHR^{MKO} mice were significantly decreased, indicating an attenuation of global inflammation (Fig. S3, K and L). Moreover, Oil Red O and H&E staining of the aorta and aortic root also showed a reduction of atherosclerosis in TSHR^{MKO} mice after a 12- and 16-wk WD diet (Fig. 4, A and B). IHC for F4/80, CCL2, and IL-6 further revealed a significant decrease in macrophage burden and inflammation in atherosclerotic plaques (Fig. 4 B). Consistently, the atherosclerotic plaques in TSHR^{MKO} mice showed significantly less involvement of middle layer and necrotic cores (Fig. S3, M and N). Taken together, these results validated that the effect of TSH on macrophages is proinflammatory and atherogenic.

As monocyte recruitment was found to be remarkably enhanced by TSH in vitro, we then tested whether monocyte recruitment was suppressed in the TSHR^{MKO} mice, by a bead labeling method (Potteaux et al., 2011) and adoptive transfer of CFSE-labeled monocytes. On one hand, significantly fewer CFSE-labeled monocytes were recovered from the aortas of TSHR^{MKO} mice 24 h after the adoptive transfer (Fig. 5 A). On the other hand, although no difference was observed in the frequency of the labeled or total monocytes in the circulation (Fig. S4, A–D), significantly fewer beads were recovered in atherosclerotic lesions of TSHR^{MKO} mice (Fig. S4 E). Consistently, a reduction in freshly recruited CD11b$^+$ CD64^{lo} Ly6C^{hi} monocytes was detected in the TSHR^{MKO} aorta by FCM (Fig. 5, C and D), accompanied by significantly fewer CD11b$^+$ CD64$^+$ macrophages (Fig. 5 E) and CD45$^+$ cells (Fig. 5 B). These results indicate that macrophage TSHR mediated TSH-induced monocyte recruitment to the plaques.

To clarify whether TSH promoted atherosclerosis by affecting macrophage apoptosis in vivo, we performed TdT dUTP nick-end labeling (TUNEL) on aortic sections of TSHR^{MKO} mice and their littermates, counterstaining F4/80 immunofluorescence. In atherosclerotic lesions, >90% of the TUNEL$^+$ cells were found to be F4/80$^+$ (data not shown), and the rate of macrophage apoptosis was not significantly different between the two groups of mice (Fig. S4 F). Moreover, the frequency of Ki67$^+$ cells, which are indicative of proliferative cells, is higher in the plaques of TSHR^{MKO} mice (Fig. S4 G) and theoretically should promote plaque growth. Therefore, accelerating proliferation should not be a mechanism by which TSH exacerbates atherogenesis.

TSH activated MAPKs and IκB/NF-κB p65 pathways in the macrophages

To reveal the mechanisms underlying the proinflammatory effect of TSH, a number of inflammation-related pathways were examined. TSH stimulation led to p65 nuclear translocation within 30 min (Fig. 6 A), inducing IκB phosphorylation and IκBα degradation in a dose- and time-dependent manner (Fig. 6, B and D). On the other hand, the phosphorylation of ERK1/2, JNKs

Table 2. **Influence of risk factors on mean CIMT**

Variable	Model 1 (R^2 = 0.253)		Model 2 (R^2 = 0.265)		Model 3 (R^2 = 0.266)	
	β[a]	P	β[a]	P	β[a]	P
Age	0.481	<0.001	0.465	<0.001	0.451	<0.001
Gender[b]	−0.056	0.033	−0.045	0.097	−0.048	0.071
TSH	0.104	<0.001	0.086	<0.001	0.082	0.002
BMI	NI	NI	0.001	0.975	−0.002	0.993
SBP	NI	NI	0.077	0.027	0.096	<0.001
DBP	NI	NI	0.043	0.208	0.046	0.164
TC	NI	NI	NI	NI	0.020	0.471
TG	NI	NI	NI	NI	0.019	0.487
LDL	NI	NI	NI	NI	0.047	0.081
HDL	NI	NI	NI	NI	-0.004	0.880
FPG	NI	NI	NI	NI	0.073	0.006

From model 1 and 2, all variables except TSH were entered into the model regardless of their significance before TSH was input with stepwise method (P < 0.10 and > 0.05 as thresholds for inclusion and exclusion). For model 3, all variables were input equally with stepwise method. BMI, body mass index; DBP, diastolic blood pressure; NI, not included as candidate variables from the beginning; SBP, systolic blood pressure.
[a]Standardized β coefficient.
[b]Male is valued as 1 and female as 2 when the variable "gender" was included as an independent.

(p46/p54) and p38α (MAPK14) were also increased by TSH treatment (Fig. 6, C and D), suggesting that MAPKs pathways were also involved in transducing TSH-induced macrophage inflammation. TSHR is solely responsible for the activation of these pathways, as *Tshr* silencing markedly blocked these effects of TSH (Fig. 6 D). By contrast, the proinflammatory effect of TSH was neglectable in endothelial cells, smooth muscle cells, and neutrophils (Fig. S5, A–C).

Discussion

Whether TSH contributes to the increased cardiovascular risk among SH patients had remained uncertain (Cappola and Ladenson, 2003; Rodondi et al., 2010; Cooper and Biondi, 2012; Delitala et al., 2017). In this study, using *Tshr*$^{-/-}$ *ApoE*$^{-/-}$ double knockout mice, the contribution of TSH to atherogenesis is observed for the first time. We further demonstrated that macrophages are an important target of the atherogenic effect of TSH, independent of the well-recognized effects of TSH on the thyroid gland and blood lipid profile.

Although in SH conditions, thyroid hormones are still within the normal range, they could be mildly decreased compared with the normal population. As metabolic alterations caused by the decline in thyroid hormones has been regarded to contribute critically to atherogenesis in hypothyroidism (Jones et al., 1955; Cappola and Ladenson, 2003), this may also be true in SH (Delitala et al., 2017). On the other hand, in SH, the most prominent biochemical change is the elevation in TSH level. Therefore, it remained yet to be determined which factor, TSH or the thyroid hormones, played a more important role in the atherosclerosis associated with SH. Actually, it is currently believed that hypothyroidism contributes to atherosclerosis mainly by altering lipid metabolism (Jones et al., 1955; Rodondi et al., 2010; Delitala et al., 2017). Interestingly, as the correlation between TSH and CIMT remained significant after adjusting lipid profile (Table 2), this suggests that the TSH is likely to contribute to atherosclerosis through some lipid- and thyroid hormone–independent mechanism. Consistently, while serum lipids (TC, TG, LDL-C, and HDL-C) and thyroid hormone levels remained constant, atherosclerosis was attenuated significantly in both global and myeloid-specific *Tshr* knockout mice.

Macrophage-related inflammation plays a critical role in atherosclerosis (Johnson and Newby, 2009; Swirski and Nahrendorf, 2013). The uncontrolled inflammation can hamper macrophage cholesterol efflux (Shibata and Glass, 2009) and efferocytosis (Sather et al., 2007) directly, leading to the accumulation of debris and enlargement of necrotic cores. Moreover, inflammatory mediators released by plaque macrophages aggravate local tissue damage, which in turn arouses more inflammation, forming a vicious circle (Johnson and Newby, 2009; Swirski and Nahrendorf, 2013). As shown by our experiments, TSH promoted macrophage inflammation and contributes to atherosclerosis directly. TSH treatment induced inflammatory cytokine production and up-regulated a series of markers indicative of acute inflammation, accompanied by the down-regulation of several critical molecules that are important for lesion resolution and reverse cholesterol transport (PPAR-γ, LXRα, and ABCA1; Fig. 3 D). Moreover, as shown by our in vivo and in vitro studies, TSH promotes monocyte recruitment to atherosclerotic plaques, leading to increased macrophage burden (Randolph, 2014). The above results suggest macrophage inflammation to be a critical target of the atherogenic effect of TSH.

In our study, increased proliferation (Fig. S4 G) and reduced monocyte recruitment (Fig. 5, A and D; and Fig. S4 E) concurred in the aortic lesion of TSHR^{MKO} mice. They likely have both played a role in regulating macrophage burden in atherosclerosis. According to previous studies, monocyte recruitment contributes more to macrophage burden in earlier stages of atherosclerosis (Robbins et al., 2013; Lhoták et al., 2016). Therefore, the effect of TSH to promote monocyte recruitment might prevail in early atherosclerosis, leading to increased macrophage burden. This is consistent with our findings that the differences in F4/80, IL-6, and CCL2 levels were stronger after 12 wk of WD compared with 16 wk (Fig. 4 B). Of note, while monocyte recruitment to TSHR^{MKO} lesions was significantly decreased after 8 wk of WD (Fig. 5, A and D), the number of Ki67^{+} cells was similar to that of LC at this stage (data not shown). As a noticeable change in macrophage burden has already taken place (Fig. 5 E), this suggests reduced monocyte recruitment to be the main cause for the reduction in macrophage burden in TSHR^{MKO} mice.

In this study, TSH was found to activate NF-κB and MAPK (ERK1/2, p38, and JNK) pathways in the macrophages. As NF-κB (Kanters et al., 2003, 2004; Goossens et al., 2011; Park et al.,

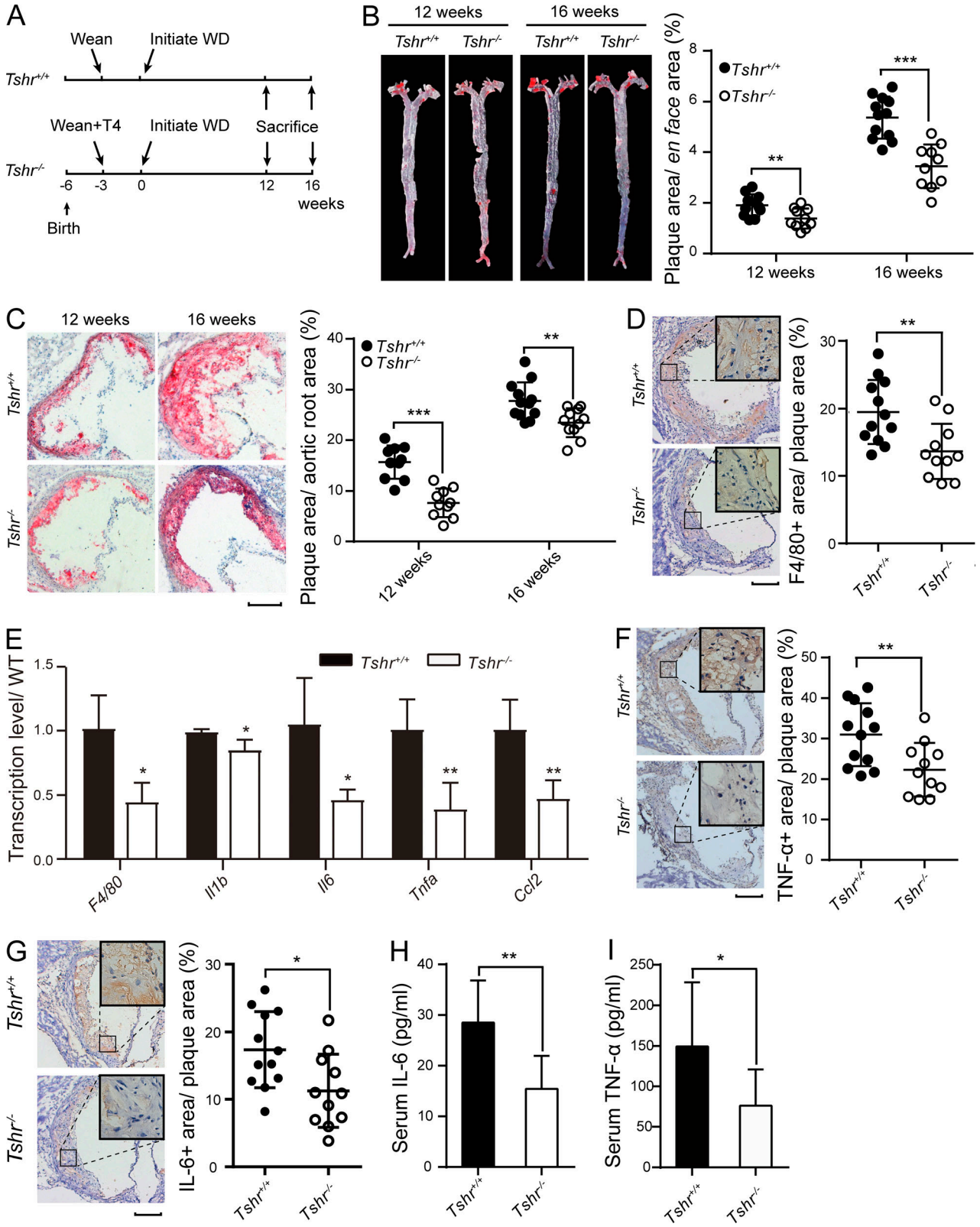

Figure 2. **TSHR knockout alleviates vascular inflammation and atherosclerosis in *ApoE*$^{-/-}$ mice. (A)** Schedule of the experiment. Diets of *Tshr*$^{-/-}$*ApoE*$^{-/-}$ mice were supplemented with thyroxine (T4) after weaning. **(B and C)** Representative Oil Red O–stained whole aorta (B) and aortic root sections (C) of the four groups of mice. **(D)** F4/80 IHC showing macrophages in aortic root lesions. **(E)** qPCR analysis of inflammatory marker expression in the aorta. Fold change of the expression level of each marker compared with *Tshr*$^{+/+}$ *ApoE*$^{-/-}$ mice (WT) is displayed. Independent experiments were repeated three times. **(F and G)** IHC of TNF-α (F) and IL-6 (G) in aortic root sections. **(H and I)** ELISA of serum IL-6 (H) and TNF-α (I) of the two genotypes. For D–I, data of mice fed WD for 16 wk are shown. Plaque area and stained area of IHC results were measured by Image-Pro Plus software. n = 10–12 (B–D, F, and G), 10–11 (H), or 13–14 (I). Data represent mean ± SD. Scale bars: 200 µm. Differences between two groups were analyzed by t test with Welch's correction, except for E, which was compared with multiple t tests using Holm–Sidak correction. *, P < 0.05; **, P < 0.01; ***, P < 0.001.

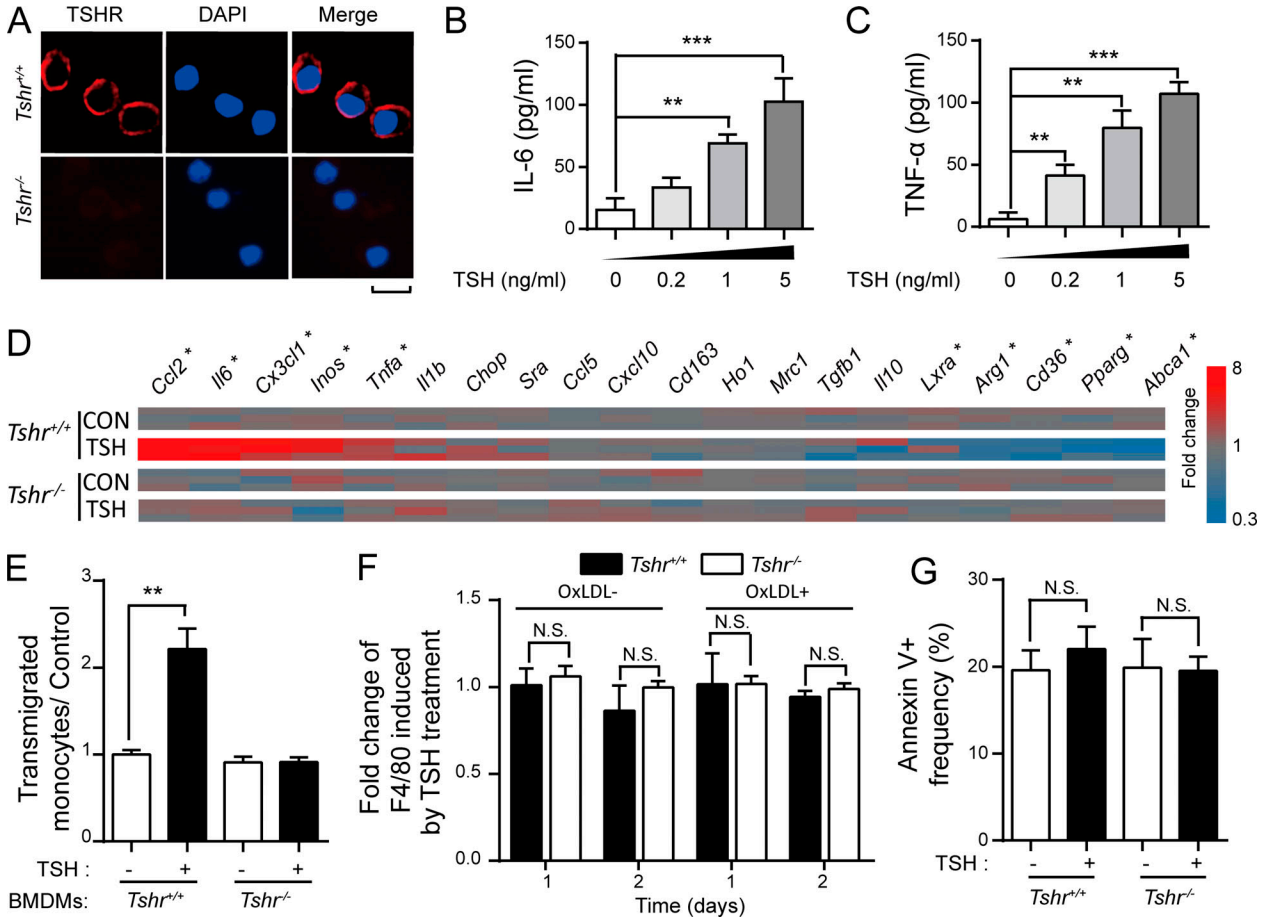

Figure 3. **TSH promoted inflammation in macrophages in vitro. (A)** TSHR immunofluorescence (red) in mouse peritoneal macrophages. Scale bar: 10 µm. **(B and C)** ELISA of IL-6 (B) and TNF-α (C) in the culture medium of mouse peritoneal macrophages, 12 h after escalating dose of TSH stimulation. **(D)** qPCR analysis of the effect of TSH on macrophage function in the presence of OxLDL. *Tshr*$^{+/+}$ or *Tshr*$^{-/-}$ BMDMs were treated with or without TSH for 24 h and further treated with 25 µg/ml OxLDL for 24 h. Asterisk, significantly affected by TSH treatment. **(E)** The effect of TSH treatment on the chemoattractive ability of the BMDM-conditioned medium in the presence of 20 µg/ml of OxLDL was studied using Transwell assay. **(F and G)** The effect of TSH on F4/80 expression during monocyte maturation (F) and macrophage apoptosis (G) was evaluated by FCM. Experiments were repeated three times. Data represent the mean ± SD. In B and C, statistical analysis was done with one-way ANOVA and post hoc Dunnett *t* test, while in D, multiple *t* tests using Holm–Sidak method were used. Differences between two groups were analyzed by *t* test with Welch's correction. **, P < 0.01; ***, P < 0.001. N.S., not significant.

2012) and MAPKs (Ricci et al., 2004; Devries-Seimon et al., 2005; Schneider et al., 2006; Kim et al., 2012; Lou et al., 2013) in macrophages are deeply intertwined in atherosclerosis, they are likely to interact extensively for the atherogenic effect of TSH. As numerous research has revealed critical roles of NF-κB and MAPKs in regulating chemokine expression (Ali et al., 2000; Shahrara et al., 2010; Carmo et al., 2014), it is very likely that MAPKs and NF-κB have cooperated to induce the expression of chemokines in the macrophages, leading to increased monocyte recruitment driven by TSH. Notably, not all their downstream genes were universally up-regulated by TSH in vitro (Fig. 3 D), and some cellular processes regulated by NF-κB and MAPKs, such as apoptosis, were not significantly altered by *Tshr* KO in vivo. This may also be a result of the complex interplay between NF-κB and MAPK pathways, as the roles of NF-κB in macrophages is versatile and highly context dependent (Medzhitov and Horng, 2009; Ivashkiv and Park, 2016). Therefore, more investigations are needed to fully uncover the detailed underlying mechanism.

It should be noted that TSH was reported to suppress IκB phosphorylation and TNF-α secretion in osteoclasts (Abe et al., 2003; Hase et al., 2006), which are other differentiated effector cells of the monocyte-macrophage system. This seemingly contradicts with our results, and several factors might have resulted in such a discrepancy. Cells of the monocyte-macrophage system are well known for their versatile phenotype and flexible function in different environments in response to different challenges (Ivashkiv, 2011; Takeuch and Akira, 2011). Therefore, macrophages under different differentiation conditions might respond differently or even oppositely to the same challenge. For example, LPS is strongly proinflammatory for quiescent macrophages, but its proinflammatory effect is not obvious in endotoxin-tolerant macrophages (Ivashkiv, 2011). Thyroxine was discovered to exert an antiinflammatory effect on macrophages, while it is proinflammatory in Kupffer cells (macrophages in the liver; De Vito et al., 2011). In Abe et al. (2003) and Hase et al. (2006), RAW cells and bone marrow macrophages were differentiated into osteoclast-like cells by sustained

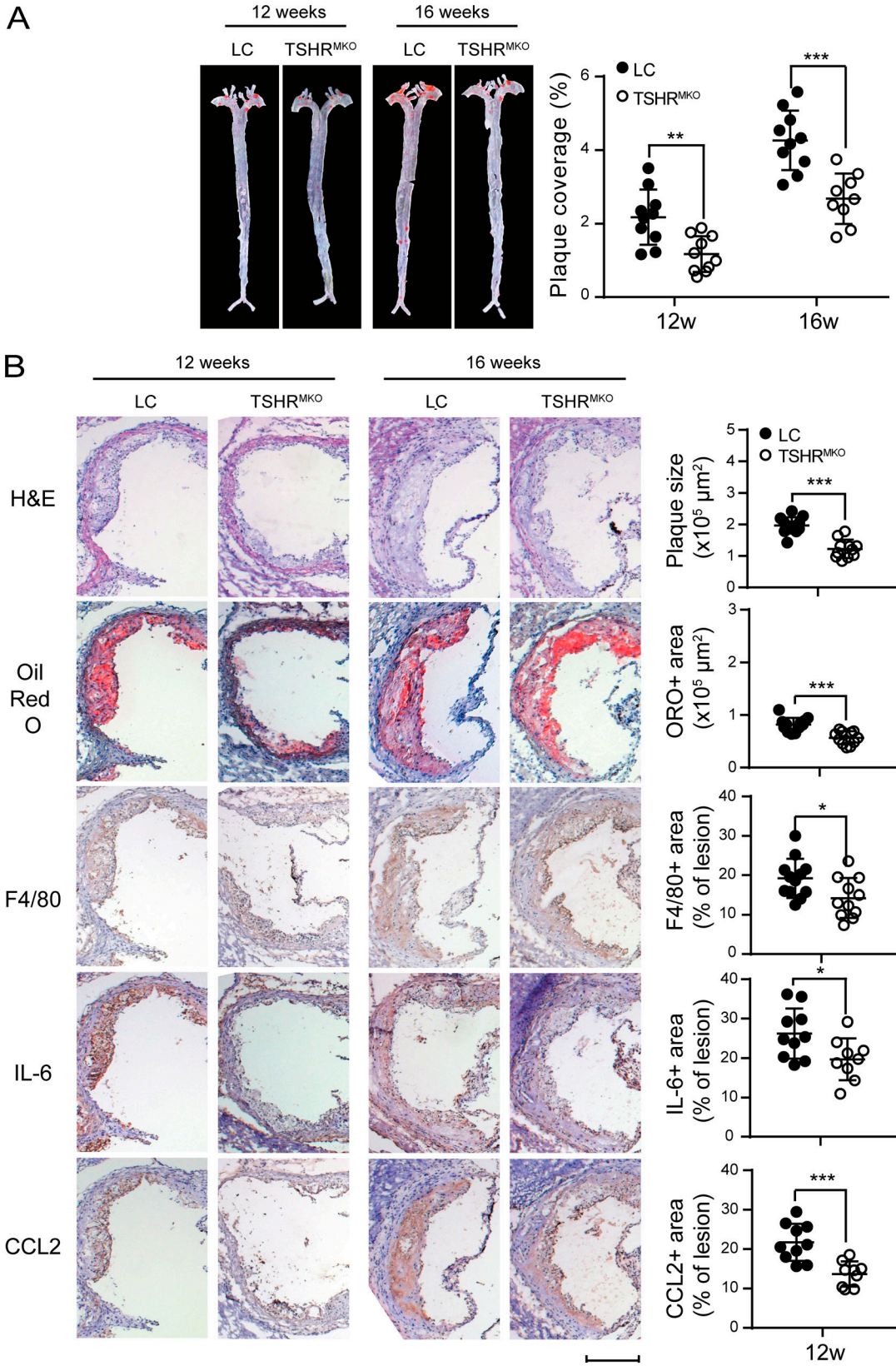

Figure 4. **Myeloid-specific TSHR knockout suppressed atherosclerosis in *ApoE*$^{-/-}$ mice. (A and B)** En face Oil Red O staining of aortas (A) and H&E, Oil Red O staining or IHC of F4/80, IL-6, and CCL2 in the aortic root sections (B) from myeloid-specific TSHR knockout mice (TSHR^{MKO}) and their littermates (LC), after 12 or 16 wk of WD. Scale bar: 200 µm. Plaque size or stained area was quantified with Image-Pro Plus software. n = 11 for mice of 12 wk and n = 9 or 10 for 16 wk. Data represent the mean ± SD. Differences between two genotypes were analyzed by t test with Welch's correction. *, P < 0.05; **, P < 0.01; ***, P < 0.001.

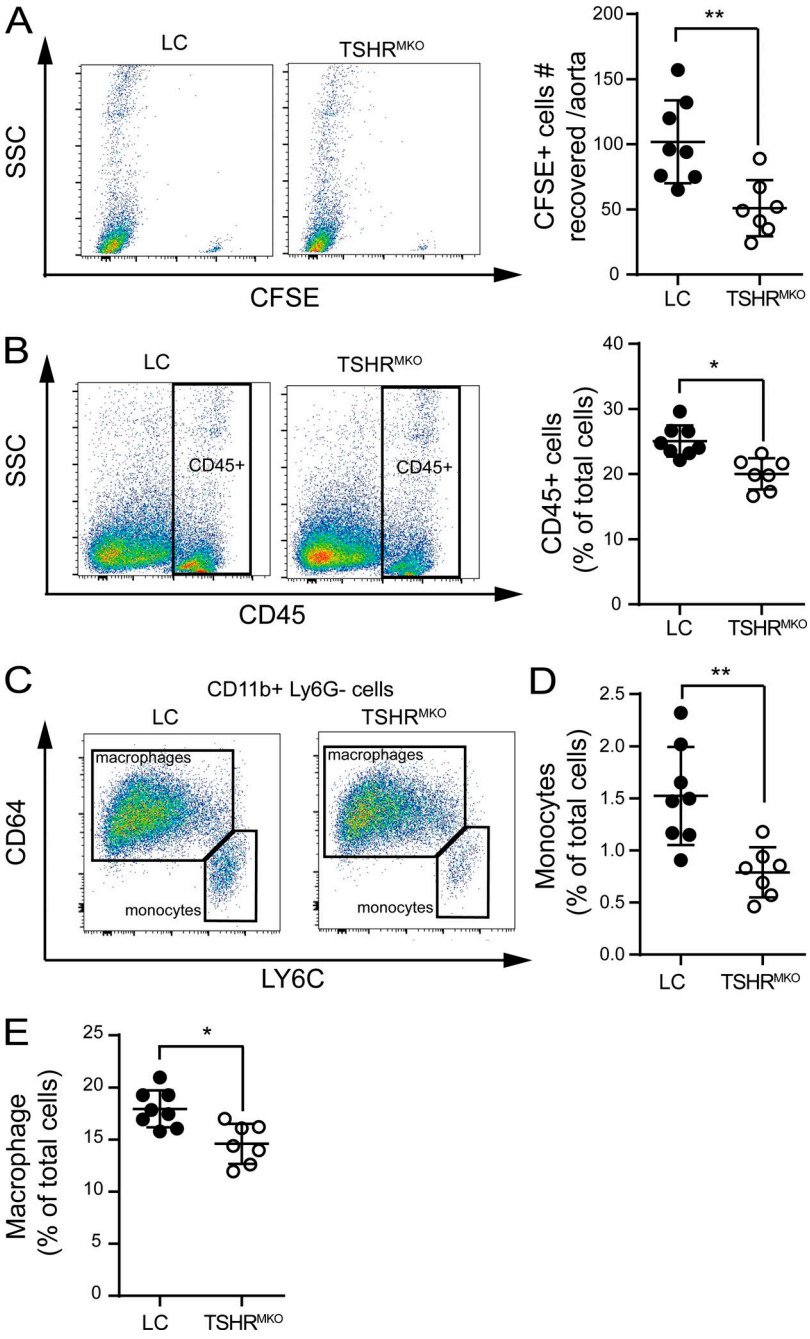

Figure 5. **Myeloid-specific TSHR knockout suppressed monocyte recruitment in atherosclerosis. (A)** Representative FCM plots and statistics showing CFSE$^+$ cells in the aorta of myeloid-specific TSHR knockout mice (TSHR^{MKO}) and their littermates (LC) 24 h after adoptive transfer of 10^6 CFSE-labeled monocytes to each mouse. **(B)** Representative FCM plots and statistics showing frequencies of CD45$^+$ cells in whole aorta detected by FCM (n = 7 or 8). **(C)** Representative FCM plot of aortic CD45$^+$ CD11b$^+$ Ly6G$^-$ cells showing how macrophages and Ly6C^{hi} monocytes were gated. **(D and E)** Frequencies of monocytes (D) and macrophages (E) in whole aorta detected by FCM. n = 7 or 8 (A–E). Data represent the mean ± SD. Differences between two genotypes were analyzed by t test with Welch's correction. *, P < 0.05; **, P < 0.01.

RANKL treatment, and therefore they might be different compared with the naive macrophages used in our study.

Although the immunomodulatory potential of TSH was reported decades ago (Kruger and Blalock, 1986; Wang et al., 1997; Bağriaçik and Klein, 2000), its physiological or pathophysiological significance remained mostly putative. In the present study, we revealed that TSH promotes macrophage inflammation and contributes to atherosclerosis directly. Our study suggests that, in the early stage of thyroid disease, the increase of TSH levels can promote global inflammation and accelerate atherosclerosis directly, apart from its effects on metabolism by regulating thyroid hormone levels. Besides atherosclerosis, a series of metabolic diseases that are driven by chronic inflammation, including obesity, insulin resistance, and hypertension, are also found to be related to TSH elevation in clinical settings (Cooper and Biondi, 2012). Therefore, whether the proinflammatory effect of TSH on macrophages also plays a role in other diseases is worth further investigation. On the other hand, aging is often accompanied by TSH elevation (Cooper and Biondi, 2012), and our discovery therefore also suggests that TSH may play important roles in the systematic changes of physical condition related to inflammation and immunity during senescence. In short, our study highlights the idea that TSH is an important regulator of immune function, which may be involved in either normal or diseased conditions.

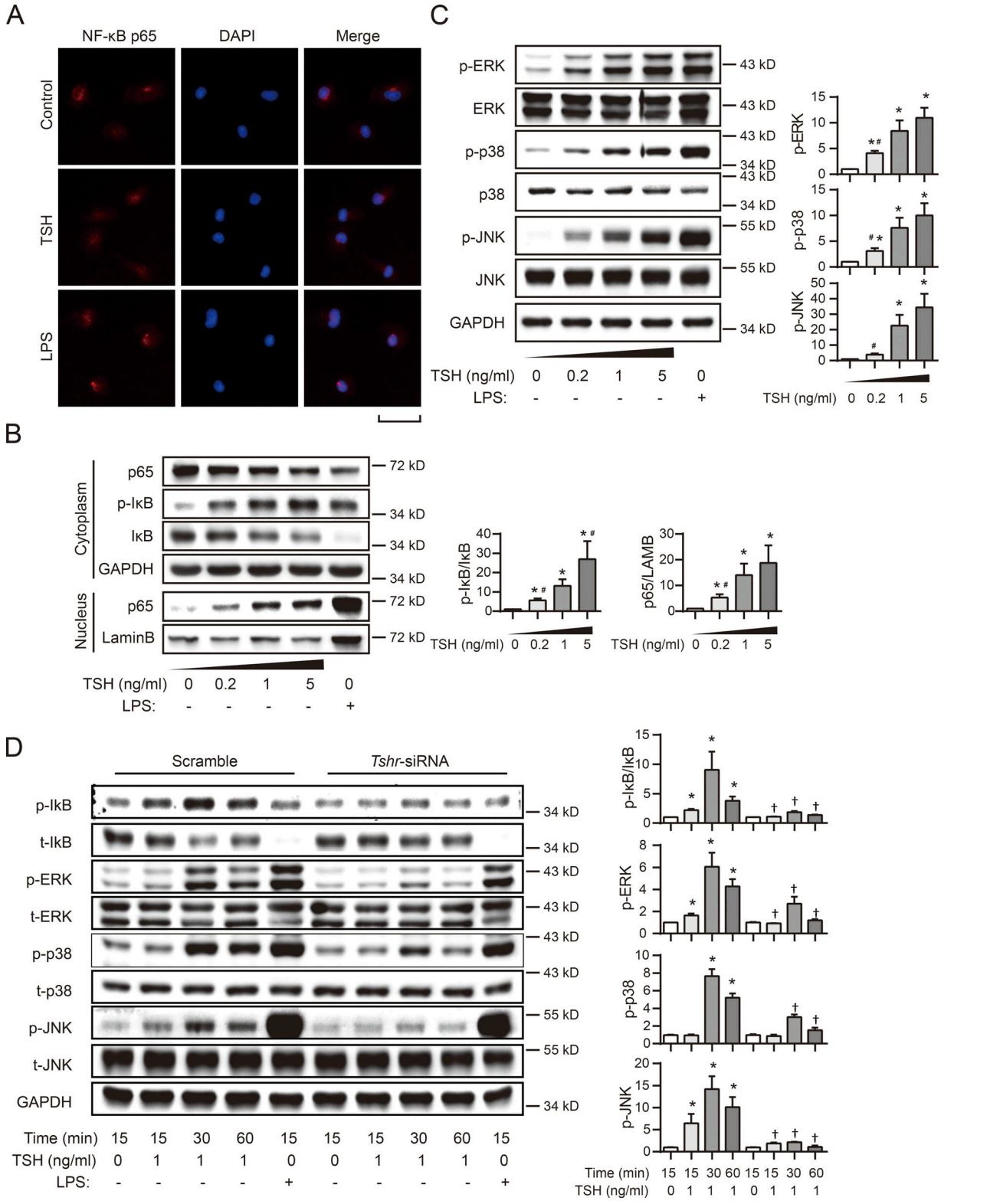

Figure 6. **TSH promoted inflammation in macrophages via IκB/NFκB and MAPKs pathway. (A)** Cellular distribution of NF-κB p65 (shown in red) 30 min after TSH treatment was visualized by immunofluorescence in mouse peritoneal macrophages. Nuclei were stained with DAPI (shown in blue). Scale bar: 20 µm. **(B and C)** Dose-dependent effects of TSH at 30 min on NF-κB pathway (B) or MAPKs (ERK1/2, p38 MAPK, and JNK) pathways (C) in RAW264.7 were examined by Western blotting. GAPDH and LAMB were used as internal references for the cytoplasmic and nuclear fractions, respectively. **(D)** The effect of TSHR silencing on the activating effects induced by TSH was evaluated by Western blotting. Control or si-*Tshr* RNA was transfected into RAW264.7 36 h before TSH treatment. For the above experiments, PBS and LPS were used as the negative and positive control, respectively. Experiments were repeated three times. Intensity of optical density of Western blotting results were measured by Image-Pro Plus software. Data represent the mean ± SD. Multigroup differences were tested with one-way ANOVA and post hoc Dunnett *t* test. *, P < 0.05 vs. control; #, P < 0.05 vs. 1 ng/ml TSH; †, P < 0.05 vs. corresponding treatment of scramble siRNA control.

It has been reported that early intervention of SH can significantly improve a patient's lipid profile (Caraccio et al., 2002; Zhao et al., 2016) and relieve atherosclerosis (Monzani et al., 2004), and our study implies that it can likely also improve outcomes by suppressing vascular inflammation. Moreover, approaches to control TSH should not be restricted to traditional methods such as thyroxine supplementation. As blocking follicular stimulating hormone (a pituitary hormone like TSH) by injection of anti–follicular stimulating hormone monoclonal antibody has been proved to have therapeutic value for obesity and metabolic diseases (Liu et al., 2017), similar anti-TSH treatment with anti-TSH monoclonal antibody is technically possible and could be devised in the future.

It should be noted that although our results obtained from $TSHR^{MKO}$ mice highlighted macrophages as critical targets of the atherogenic effect of TSH, LyzCRE-mediated deletion can also affects myeloid cells other than macrophages, such as monocytes and neutrophils, which might have confounded the end points. However, the effect of TSH on monocytes or neutrophils may not play an important role in atherosclerosis, given that TSH does not activate neutrophils (Kiss et al., 1997; Marino et al., 2006; Fig. S5 C) or promote monocyte recruitment by acting on monocytes directly (Fig. S2 D), and no significant change in neutrophil or monocyte frequency was observed in the circulation of $TSHR^{MKO}$ mice (Fig. S4 D). Nevertheless, although the reduction in atherosclerotic lesions in $TSHR^{MKO}$ mice was found to be comparable to that in global *Tshr* knockout mice, we cannot completely exclude the possibility that the effects of TSH on other cells also influence atherogenesis. Therefore, more delicate investigations are needed for a complete understanding of the role of TSH in atherosclerosis.

In conclusion, based on the studies performed in the population, in gene knockout mice, and in vitro, we demonstrate that TSH can contribute to atherogenesis directly by promoting macrophage inflammation in atherosclerotic plaques (Fig. 7). This study modifies the current understanding of how SH increases cardiovascular risk and reveals TSH as a potential target for both the prevention and the treatment of cardiovascular diseases, and possibly other inflammatory diseases.

Materials and methods

Human subjects: Inclusion and exclusion criteria and measurements

The epidemiological data were obtained from our long-term follow-up research center in Ningyang, Shandong Province, China. 2,480 participants were involved in the study. The sample size of the epidemiological study is based on a previous population-based study focused on SH (Hak et al., 2000). All participants signed consent forms, and the Ethics Committee of Shandong Provincial Hospital approved this study. All of the participants underwent a standard examination in the morning including the following: a detailed medical history inquiry; measurement of blood pressure, height, and body weight; collection of fasted serum sample for measurement of serum levels of TC, TG, HDL-C, LDL-C, FPG, and inflammation markers. Anthropometric parameters, such as sex, age, marital status, smoking status, and other essential information were obtained via questionnaire. Blood samples were collected from subjects who had fasted for ≥10 h. Thyroid function was assessed by serum levels of TSH, FT3, and FT4, using chemiluminescent methods (Cobas E601; Roche). The levels of fasting blood glucose (FBG), TC, TG, LDL-C, and HDL-C were measured using a Olympus AU5400 system. Individuals with previous thyroid disease and its treatment (antithyroid medications, thyroid hormone, thyroidectomy, or radiodine therapy), positive cardiovascular event history, diabetes mellitus, hypertension, medications known to affect lipid profile (e.g., statin), malignant tumor, chronic liver diseases, chronic kidney diseases, and/or abnormal FT4 level (i.e., <11.5 or >22.7 pmol/liter) were excluded (Hak et al., 2000; Cooper and Biondi, 2012), and the remaining 1,103 participants were classified into three groups according their TSH levels (Table 1; Cooper and Biondi, 2012). For inflammation marker quantification, subjects were selected from each group by a random number generation method. Serum TNF-α was quantified with a human TNF-α ELISA kit (Invitrogen), and other inflammatory markers in their serum were quantified using a customized Human Magnetic Luminex Assay kit (R&D Systems) and a Luminex 200 system.

Carotid ultrasonography

CIMT was measured by ultrasound according to the current sonographic guidelines (Touboul et al., 2012). Briefly, CIMT in all patients was measured using a color ultrasound system equipped with a 9-MHz linear-array transducer (Toshiba Aplio 500 Ultrasound Scanner). The anterior, posterior, and medial IMT of the carotid on both sides were each measured three times, and the mean of all the measurements (18 values) was calculated and taken as the CIMT of each individual. Focal structures encroaching into the arterial lumen of ≥0.5 mm or 50% of the surrounding IMT value and/or IMT >1.5 mm was indicative of the presence of atherosclerotic plaque. For each subject, a continuous scan of bilateral carotid arteries, starting from the origin of carotid artery (right, cephalobrachial trunk; left, aortic arch) to where the internal and external carotid arteries become unrecognizable, was performed to identify carotid atherosclerotic lesions. The same investigator who was blinded to the patients' clinical data performed each scan.

Animals, genotypes, and diet

$Tshr^{-/-}ApoE^{-/-}$ and their $Tshr^{+/+}ApoE^{-/-}$ littermate mice were generated by crossbreeding $ApoE^{-/-}$ mice (The Jackson Laboratory) with $Tshr^{+/-}$ mice (The Jackson Laboratory). $Tshr^{-/-}ApoE^{-/-}$ mice were fed the aforementioned diet containing 100 ppm thyroid powder (Marians et al., 2002; containing ∼15 µg of T4 per kg of diet; Sigma) in addition from the age of 21 d to maintain the physiological level of thyroxine.

Conditional *Tshr* ablation was achieved with a CRE recombinase-based system, by crossbreeding $Tshr^{flox/flox}$ mice (Cyagen Biosciences) with $LyzCre^{+}$ mice (a mouse strain with myeloid-specific CRE expression; The Jackson Laboratory). To induce atherosclerosis, *LyzM-Cre* $Tshr^{flox/flox}$ mice were subsequently crossed into $ApoE^{-/-}$ background, yielding *LyzM-cre*$^{+}$ $Tshr^{flox/flox}$ $ApoE^{-/-}$ ($TSHR^{MKO}$) mice, and their $LyzCre^{+}$ $ApoE^{-/-}$ littermates were used as controls (LC). The $LyzCre^{+}$ $Tshr^{flox/+}$ $ApoE^{-/-}$ mice were used for continuous breeding.

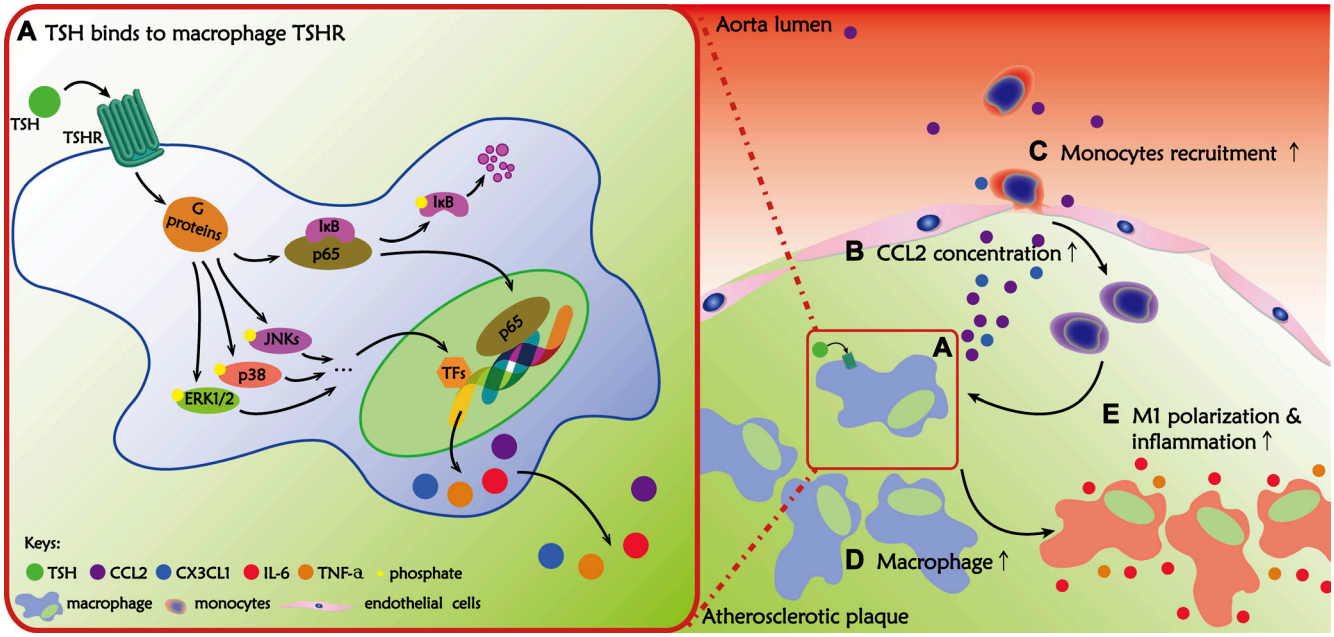

Figure 7. **TSH promotes atherosclerosis by acting on macrophages.** Left: By binding to macrophage TSHR, TSH activated IκB/NF-κB and MAPK pathways, induced the expression and secretion of chemokines (CCL2 and CX3CL1) and other inflammatory cytokines (IL-6 and TNF-α). Right: The increase in chemokine concentration in the plaque promoted monocyte recruitment, and the increase in inflammatory cytokines led to more propagated and sustained inflammation.

All animals used for the experiments were either of >98% C57 background when purchased or backcrossed at least five generations, were confirmed to have 98% C57BL/6 genetic background by genome-wide SNP analysis, and were maintained in standard animal facilities. Male mice were used for all experiments in this study. No randomization of animals was used in this study. To accelerate atherosclerosis development, the above model mice were fed a WD (2% cholesterol and 15% saturated fatty acid) from 6 wk of age and sacrificed 12 or 16 wk afterwards, and their anticoagulated blood, serum, whole aorta, and aortic root samples were collected. Serum TC, TG, HDL-C, and LDL-C were tested with enzymatic methods on an Olympus AU5400 system. Serum levels of total T4 and TSH were measured, respectively, using a radioimmunoassay kit (Jiuding Tianjing Biomedical Engineering Co.) and an ELISA kit (myBiosource). On harvest, each sample was assigned an analytical code that was irrelevant to its genotype and processed and analyzed by a researcher blinded to its origin. The animal experimental protocol conformed to the *US Department of Health and Human Services Guide for the Care and Use of Laboratory Animals* and was approved by the Animal Ethics Committee of Shandong Provincial Hospital.

En face Oil Red O staining of whole aorta

The whole aortas (from the aortic arch to the iliac bifurcation) of mice were fixed with 4% polyformaldehyde overnight and then immersed in PBS for 1 d. After fat removal, aortas were washed twice with 78% (vol/vol) methanol, stained for 1 h with Oil Red O staining solution (Goodbio Technology), and differentiated twice with 78% (vol/vol) methanol, for 5 min each time. Residual fat was then removed, and the aorta was cut open longitudinally before being photographed using a Canon E60 camera with a fixed photographic program. The total and atherosclerotic lesion areas of each aorta were measured with Image Pro Plus software, version 6.0 (Media Cybernetics).

Aortic root lesion analysis

For aortic root cross-section analysis, the aortic roots were excised from mice, covered in optimal cutting temperature compound, and frozen in liquid nitrogen. On harvest, a sample number that was irrelevant to the tag number or genotype of the mouse was given to each sample, and the downstream procedures were performed by personnel blinded to the origin of these samples. The sections were sectioned with a cryostat (CM1950; Leica) from the apex to the base in 6 µm, collected continuously onto 10 slides when three valves concurred in the arterial lumen, and stored at −80°C. For each sample, five to six sections on one slide were used for staining and analysis. Standard procedures were used for the H&E, Oil Red O, and Sirius Red staining of the aortic root sections. For IHC, slides were brought to room temperature (RT), fixed with 4% polyformaldehyde, blocked with 3% hydrogen peroxide and 10% goat serum, and incubated with the corresponding primary antibody (anti-mouse F4/80 monoclonal antibody [clone CI:A3-1; Abcam], anti-mouse CCL2 antibody [clone ECE.2; Abcam], anti-Ki67 antibody [clone SP6; Abcam], anti-iNOS [clone 136918; Abcam], anti–IL-6 polyclonal antibody [Proteintech], anti–TNF-α polyclonal antibody [Proteintech], anti-MOMA antibody [clone MOMA-2; Abcam], and anti–α-SMA [clone E184; Abcam]) at 4°C overnight. The antibodies were then detected with a Polink-1 HRP detection system (ZSGB Bio). Isotype IgG were used as negative controls. All sections were examined by Axio Imager A2 (Carl Zeiss), and pictures were acquired with an AxioCam HRc camera (Carl Zeiss,) using Axiovision release 4.8 software. Photos were analyzed with software Image Pro Plus 6.0 (Media Cybernetics). For Ki67

staining analysis, Ki67$^+$ cells of each section were counted directly under the microscope and normalized to plaque size measured from the corresponding sections that had been stained with H&E.

TUNEL of aortic root section

Slides were brought to RT, fixed with 4% polyformaldehyde, blocked with 10% goat serum, and incubated with anti-mouse F4/80 monoclonal antibody and subsequently with TRITC-labeled goat anti-rat IgG (ZSGB Bio). After washing with PBS, slides were fixed another time with 4% polyformaldehyde, and TUNEL was performed using the in situ cell death detection kit (Roche), following the instructions provided by the manufacturer. Staining was observed and photographed under a confocal microscope (E780; Carl Zeiss). TUNEL$^+$ cells were counted manually under the microscope and normalized to cell count of the corresponding section.

FCM of mouse whole aorta

FCM analysis of mouse aorta was performed as described (Galkina et al., 2006). Briefly, whole aorta was microdissected from mice after sufficient cardiac perfusion with heparinized PBS. Rinsed with PBS, each aorta was cut briefly with fine scissors and digested in 2 ml PBS containing 550 U/ml collagenase I, 120 U/ml collagenase XI, 60 U/ml hyaluronidase, and 60 U/ml DNase (Sigma-Aldrich), at 37°C for 1 h on a magnetic stirrer. The suspensions were filtered with 70-µm cell strainers, and the unfiltered tissue was minced with a syringe plunger and washed with PBS. Cells were washed with PBS, Fc-blocked with rat anti-mouse CD16/CD32 (BD PharMingen), and incubated in staining buffer (BD Bioscience) containing antibodies (anti-CD45-APCH7 [30-F11], anti-CD64-APC [X54-5/7.1], anti-Ly6C-PECy7 [HK1.4], anti-CD11b-PERCP-Cy5.5 [M1/70], and anti-Ly6G-PE [1A8-ly6g]; Moore et al., 2013) for 45 min on ice, protected from light. Washed once with PBS, samples were analyzed by a flow cytometer (LSR Fortessa II; BD Bioscience). Isotype and FMO staining were used to determine the positively stained populations. After excluding multiplets and debris, CD45$^+$ CD11b$^+$ Ly6G$^-$ cells were gated for the analysis of macrophage and monocyte populations. Frequencies of cells were normalized to events included in the forward/side scatter gate. Plots were made using the software FlowJo vX (TreeStar).

Monocyte in vivo labeling with fluorescent beads

The procedure of in vivo monocyte labeling was detailed in Potteaux et al. (2011). Briefly, 1 µm Fluoresbrite (Polyscience) was diluted 1:24 in PBS and injected 250 µl per mice i.v. 5 d before euthanasia. EDTA-anticoagulated blood was obtained, stained with anti-CD115-APC, and subjected to FCM to monitor the specificity and efficiency of the labeling. Aortic root sections obtained as described above were stained with DAPI and observed under the microscope. Beads recovered in each section were counted manually under the microscope.

FCM of murine peripheral blood

30 µl of freshly obtained EDTA-anticoagulated blood was added with anti-mouse CD45-APC-eFlour780 (clone 30-F11), CD115-APC (clone AFS98), Gr-1-FITC (clone RB6-8C5), CD3e-PE (clone 145-2C11), and CD19-PE-Cy7 (clone eBio1D3) and incubated on ice for 40 min in the dark. Cells were then added with 1 ml of RBC lysis buffer (0.155 M NH_4Cl, 0.01 M $KHCO_3$, and 0.1 mM EDTA) and incubated for 10 min at RT. Cells were then washed two times with PBS and analyzed with a flow cytometer (LSR Fortessa II). Plots were made using the software FlowJo vX.

Adoptive transfer of CFSE-labeled monocytes

Monocytes were isolated from the peripheral blood of C57/BL6 mice with a negative magnetic sorting kit (EasySep murine monocyte isolation kit; Stemcell) following the kit instructions. The purity of the isolated cells were tested by FCM to be >95% (CD115$^+$ Ly6G$^-$). After isolation, the monocytes were labeled by incubating in PBS containing 5 µM CFSE (34554; Thermo Fisher Scientific) and 2 mM EDTA at 37°C for 10 min. Each recipient mice ($TSHR^{MKO}$ mice or LC fed 8 wk of WD) were then injected i.v. with 10^6 labeled monocytes and executed 24 h later for FCM analysis of the whole aorta.

Primary cell culture and treatment of macrophages in vitro

Mouse peritoneal macrophages

Mouse peritoneal macrophages were harvested by peritoneal lavage of 3% starch solution i.p. injected in C57/BL6 mice, seeded 2×10^6 cells/ml onto 24-well plates, and maintained with regular culture medium (RPMI 1640 [Gibco] containing 10% heat-inactivated FBS [Gibco] supplemented with 20 µM glutamine). After overnight incubation, nonadherent cells were removed, and adherent cells were used as macrophages. Cells were added with 0.2, 1, or 5 ng/ml recombinant mouse TSH (R&D Systems) and incubated for 12 h before the culture media were harvested and their IL-6 or TNF-α concentrations quantified with mouse TNF-α Platinum ELISA kit or mouse IL-6 ELISA kit high sensitivity (eBioscience) according to the instructions provided. Total cytokine production of each sample was calculated as the multiplication of concentration times the total volume of the medium harvested. Relative cytokine production of each sample to the nontreated control was calculated for graphing and analysis.

BMDMs and bone marrow monocytes and neutrophils

BMDMs were obtained by culturing the bone marrow cells harvested from the humerus, femurs, and tibias of *Tshr*$^{+/+}$ or *Tshr*$^{-/-}$ mice (16–20 wk old), in the differentiation medium (regular culture medium supplemented with 30 ng/ml M-CSF [eBioscience]) for 7 d. To study the impact of TSH on macrophage function, BMDMs were treated with 0.5 ng/ml TSH for 24 h and then incubated for another 24 h after addition of 25 µg/ml of OxLDL (Peking Union-Biology), before being harvested for quantitative PCR (qPCR) analysis. To study the effect of TSH on macrophage apoptosis, BMDMs were cultured in 24-well plates, 80 µg/ml of OxLDL was added after the first 24 h of TSH treatment, and cells were detached with Accutase (eBioscience) and stained with PI/Annexin V cell apoptosis detection Kit (BD Bioscience) according to the provided protocol. Murine monocytes were obtained from bone marrow using a negative magnetic sorting kit (EasySep murine monocyte isolation kit; Stemcell), following the instructions provided by the manufacturer. The freshly isolated monocytes were then used for Transwell assay

or differentiation study. In the differentiation study, monocytes were seeded at a density of 10^6 cells/ml in 48-well plates and differentiated in the presence or absence of 0.5 ng/ml TSH. Another half of monocytes were differentiated in the presence of 20 µg/ml OxLDL. On the first and second days after seeding, cells were harvested by Accutase digestion, stained with F4/80-PE, and analyzed by FCM. BMDMs from *Tshr*$^{+/+}$ or *Tshr*$^{-/-}$ mice were also used to study the effect of TSH on macrophage differentiation. In these experiments, BMDMs were harvested on the first, third, fifth, or seventh day of differentiation for qPCR analysis of differentiation marker expression. Neutrophils were isolated from bone marrow cells with a density-gradient based kit (TBDscience).

RAW264.7 monocyte-macrophages

RAW264.7 macrophage cells were used for the in vitro study of the inflammatory response of macrophages. In this study, authenticated RAW264.7 were obtained from ATCC, maintained in DMEM (Hyclone) containing 10% FBS (Tianhang Biotechnology) and 20 µM glutamine under humidified conditions at 37°C and 5% CO_2 in an incubator, passaged with the protocol provided by ATCC, and used for most of the pathway analysis in this article. To reveal the time-dependent effects of TSH, RAW264.7 cells were stimulated with 1 ng/ml TSH for 15, 30, or 60 min; for dose-dependent effects, RAW264.7 cells were stimulated for 30 min with 0.2, 1, or 5 ng/ml TSH. In the above experiments, an equal volume of PBS was added as negative control for TSH treatments, and in some of the experiments, 50 ng/ml LPS was used as positive control.

TSHR immunofluorescence staining

Cryosections of aortic root were prepared as described above. For detecting TSHR in the plaque, sections were fixed for 30 min with 4% polyformaldehyde at RT, blocked for 1 h with 5% goat serum at RT, incubated overnight with anti-TSHR antibody (TA321116; Origene) and anti-MOMA antibody (clone MOMA-2; Abcam), and detected on the next day with secondary antibodies (goat anti-rabbit IgG-Alexa Fluor 647 and goat anti-rat IgG-Alexa Fluor 555; 150083 and 150158; Abcam). Nuclei were stained with DAPI. For detecting TSHR in mouse peritoneal macrophages, cells were obtained as described above, seeded to 35-mm Petri dishes containing imaging glass slides, and cultured overnight in the cell incubator. The slides were then fixed for 30 min with 4% polyformaldehyde at RT, blocked for 1 h with 5% donkey serum diluted in PBS, incubated with anti-TSHR Ab (N-19) or isotype IgG (Santa Cruz Biotechnology) diluted in blocking solution overnight at 4°C, and detected with secondary antibody (Rb anti-goat TRITC) on the next day.

Transwell assay

Before the assay, the culture medium of *Tshr*$^{+/+}$ or *Tshr*$^{-/-}$ BMDMs were replaced with assay buffer (RPMI 1640 containing 1% BSA and 10 ng/ml M-CSF) containing 25 µg/ml OxLDL and treated with 0.5 ng/ml TSH or an equal volume of PBS for 12 h. After the incubation, the supernatant of the assay buffer was collected and placed to the lower chamber of the 24-well Transwell plate equipped with 3-µm polyporous polycarbonate membrane inserts. In another case, assay buffer containing 1 ng/ml TSH, 50 µg/ml OxLDL, 10% FBS, or 50 ng/ml CCL2 (Sinobiological) was placed in the lower chamber instead of BMDM conditioned assay buffer to study the chemoattractive ability of these molecules. Freshly isolated *Tshr*$^{+/+}$ murine monocytes were resuspended with the assay buffer in a density of 2 × 10^6 cells/ml and 100 µl added to each insert. The plate was incubated for 3 h in the tissue culture incubator. Afterwards, the inserts were carefully removed, and the plate was centrifuged at 500 *g* for 5 min with a swing bucket rotor. With supernatant removed, the plate was then allowed to dry overnight at RT, fixed with 4% polyformaldehyde, stained with DAPI, and observed under an inverted microscope (DMI 4000B; Leica) with a 10× objective. For each well, most crowded fields (usually at the center of the population) were photographed, and the cells were counted by Image Pro Plus software.

TSHR siRNA interference

siRNA interference of *Tshr* in RAW264.7 was performed 36 h before TSH treatment using jetPRIME reagent (PolyPlus) according to the instructions provided by the manufacturer. 50 nmol of *Tshr* siRNA (sense: 5′-ACCAGAAGCUUAACCUAUA-3′; anti-sense: 5′-GUACAACAAUGGAUUUACU-3′) purchased from GenePharma was used.

RNA extraction and real-time PCR

For RNA extraction from aortas, perivascular fat was removed carefully when aortas were excised from mice. The aortas were washed briefly in PBS, snap frozen with liquid nitrogen, grinded quickly, and dissolved with 1 ml RNAiso Plus (Takara Bio). For RNA extraction from cultured cells, cells were scraped off the plate after RNAiso Plus was added. RNA was quantified with a Nanodrop 2000 (Thermo Fisher Scientific), and 1 µg of total RNA from each sample was used as the template in a 20-µl retrotranscriptional system using Primescript RT Reagent kit (Perfect Real Time; Takara Bio) according to the manufacturer's instructions. The qPCR for specific genes was performed using Bestar qPCR SYBR Green Master Mix (DBI Bioscience) on a Light Cycler480 (Roche Diagnostics). All primers used are intron spanning, and the housekeeping gene *Actb* was used as internal standard. Cq values for each reaction were determined using second derivative maximum method, and the amplification efficiency was presumed to be 2 for fold-change calculation. Sequence information of the qPCR primers used in this study is listed in Table S1.

Western blot analysis

Protein extraction from aortic tissue was done as previously described (Rivera-Torres, 2015). The cytosol and nuclear protein were obtained using Nuclear and Cytoplasmic Protein Extraction kit (CWBIO) according to the manufacturer's instructions. Proteins were separated by SDS-PAGE and transferred electrophoretically to polyvinylidene fluoride membranes (Millipore). After blocking with 5% nonfat milk in TBST (pH 7.4, 20 mM Tris-HCl, 15 m NaCl, and 0.1% [vol/vol] Tween-20), the membranes were incubated overnight at 4°C with primary antibodies as follows: anti-TSH (bs-2676R) from Bioss; anti–NF-κB p65 (ab32536, clone E379), anti-IκBα (ab32518, E130) from Abcam; anti–p-IκBα (CST9246, clone 5A5), anti–p-Thr202/Tyr204 Erk1,2 (CST4695,

clone 137F5), anti-t-ERK (CST4376, clone 20G11), anti-p-Thr180/Tyr182 p38MAPK (CST4511, clone D3F9), anti-t-p38 (CST9228, clone L53F8), anti-p-Thr183/Tyr185 JNK (CST4668 clone 81E11) from Cell Signaling Technology; anti-t-JNK (sc-7345, clone D-2) from Santa Cruz Biotechnology; and anti-GAPDH, (60004-1-ig, clone 1E6D9) and anti-laminin B (66095-1-ig, clone 3C10G12) from Proteintech. After washing with TBST, the membranes were incubated for 1 h at 25°C with the appropriate HRP-conjugated secondary antibody. The bands were visualized by FluorChemQ system using a chemiluminescence kit (Pierce).

Statistical analysis

Quantitative variables were expressed as the mean ± SD unless stated otherwise. Multiple group comparisons were done by one-way ANOVA followed by post hoc Bonferroni or Dunnett *t* test unless stated otherwise. Comparisons between two groups were made with *t* test with Welch's correction, and two-sided $P \le 0.05$ was considered significant. When multiple comparisons were made between two groups, Holm–Sidak adjustment was used. Multivariate linear regression was used to study the relative contribution of traditional vascular risk factors (age, gender, etc.) and TSH to CIMT. The forward stepwise method was used with $P < 0.10$ and 0.05 as thresholds for inclusion and exclusion of variables, respectively. Nominal variables were compared with χ^2 or Fisher's exact test when appropriate. Epidemiological data were analyzed with SPSS v.22.0 (IBM), while experimental data were analyzed with Prism 6.0 (GraphPad).

Online supplemental material

Fig. S1 includes evidence for the presence of TSH in plaques and additional data related to Fig. 2, showing similar metabolic parameters of *Tshr*$^{-/-}$*ApoE*$^{-/-}$ mice and *Tshr*$^{+/+}$*ApoE*$^{-/-}$ mice. Fig. S2 includes evidence for the expression of TSHR in plaque macrophages and additional data related to Fig. 3, showing the setting of Transwell study and similar differentiation of *Tshr*$^{-/-}$ and *Tshr*$^{+/+}$ bone marrow cells toward macrophages. Fig. S3 includes the illustration and confirmation of the CRE-flox system in TSHR^{MKO} mice and additional data related to Fig. 4, showing similar metabolic parameters yet different cytokine levels between TSHR^{MKO} mice and LC. Fig. S4 includes additional data related to Fig. 4, examining the specificity and efficiency of in vivo bead labeling, showing rate of apoptosis and Ki67^{+} cells in TSHR^{MKO} plaque compared with LC. Fig. S5 includes Western blotting of IκB showing the effect of TSH on in endothelial cells, smooth muscle cells, and neutrophils.

Acknowledgments

We thank Professors Dianqing Wu, Lin Li, and Mansen Wang for their insightful comments. We also thank Haizhu (Zita) Yang for her assistance in the artwork.

This research was supported by grants from the National Basic Research Program (2012CB524900), the National Natural Science Foundation of China (81230018, 81170794, 81430020 [to J. Zhao], 81500595, 91439111, 81770774, 31471321, 81670721), and Shandong Provincial Natural Science Foundation (JQ201519, 2014ZRQ003).

The authors declare no competing financial interests.

Author contributions: J. Zhao defined the research theme. L. Gao, Hongjia Zhang, and Q. Zhang guided the research experiments and/or paper writing. M. Lu and C. Yang performed experiments, collected and analyzed the data, and wrote the paper. W. Jiang, Haiqing Zhang, X. Zhou, and M. Zhao did the clinical data collection. Y. Yu performed the ultrasonography. W. Chen and T. Bo designed the Cre-Loxp mouse model. M. Feng did FCM. Z. He, X. Hou, L. Wang, and C. Yu performed data analysis.

Submitted: 1 August 2018
Revised: 7 January 2019
Accepted: 11 February 2019

References

Abe, E., R.C. Marians, W. Yu, X.B. Wu, T. Ando, Y. Li, J. Iqbal, L. Eldeiry, G. Rajendren, H.C. Blair, et al. 2003. TSH is a negative regulator of skeletal remodeling. *Cell.* 115:151–162. https://doi.org/10.1016/S0092-8674(03)00771-2

Ali, H., J. Ahamed, C. Hernandez-Munain, J.L. Baron, M.S. Krangel, and D.D. Patel. 2000. Chemokine production by G protein-coupled receptor activation in a human mast cell line: roles of extracellular signal-regulated kinase and NFAT. *J. Immunol.* 165:7215–7223. https://doi.org/10.4049/jimmunol.165.12.7215

Bağriaçik, E.U., and J.R. Klein. 2000. The thyrotropin (thyroid-stimulating hormone) receptor is expressed on murine dendritic cells and on a subset of CD45RBhigh lymph node T cells: functional role for thyroid-stimulating hormone during immune activation. *J. Immunol.* 164:6158–6165. https://doi.org/10.4049/jimmunol.164.12.6158

Bis, J.C., M. Kavousi, N. Franceschini, A. Isaacs, G.R. Abecasis, U. Schminke, W.S. Post, A.V. Smith, L.A. Cupples, H.S. Markus, et al.; CARDIoGRAM Consortium. 2011. Meta-analysis of genome-wide association studies from the CHARGE consortium identifies common variants associated with carotid intima media thickness and plaque. *Nat. Genet.* 43:940–947. https://doi.org/10.1038/ng.920

Cappola, A.R., and P.W. Ladenson. 2003. Hypothyroidism and atherosclerosis. *J. Clin. Endocrinol. Metab.* 88:2438–2444. https://doi.org/10.1210/jc.2003-030398

Caraccio, N., E. Ferrannini, and F. Monzani. 2002. Lipoprotein profile in subclinical hypothyroidism: response to levothyroxine replacement, a randomized placebo-controlled study. *J. Clin. Endocrinol. Metab.* 87:1533–1538. https://doi.org/10.1210/jcem.87.4.8378

Carmo, A.A., B.R. Costa, J.P. Vago, L.C. de Oliveira, L.P. Tavares, C.R. Nogueira, A.L. Ribeiro, C.C. Garcia, A.S. Barbosa, B.S. Brasil, et al. 2014. Plasmin induces in vivo monocyte recruitment through protease-activated receptor-1-, MEK/ERK-, and CCR2-mediated signaling. *J. Immunol.* 193:3654–3663. https://doi.org/10.4049/jimmunol.1400334

Collet, T.H., D.C. Bauer, A.R. Cappola, B.O. Asvold, S. Weiler, E. Vittinghoff, J. Gussekloo, A. Bremner, W.P. den Elzen, R.M. Maciel, et al.; Thyroid Studies Collaboration. 2014. Thyroid antibody status, subclinical hypothyroidism, and the risk of coronary heart disease: an individual participant data analysis. *J. Clin. Endocrinol. Metab.* 99:3353–3362. https://doi.org/10.1210/jc.2014-1250

Cooper, D.S., and B. Biondi. 2012. Subclinical thyroid disease. *Lancet.* 379:1142–1154. https://doi.org/10.1016/S0140-6736(11)60276-6

Delitala, A.P., G. Fanciulli, M. Maioli, and G. Delitala. 2017. Subclinical hypothyroidism, lipid metabolism and cardiovascular disease. *Eur. J. Intern. Med.* 38:17–24. https://doi.org/10.1016/j.ejim.2016.12.015

De Vito, P., S. Incerpi, J.Z. Pedersen, P. Luly, F.B. Davis, and P.J. Davis. 2011. Thyroid hormones as modulators of immune activities at the cellular level. *Thyroid.* 21:879–890. https://doi.org/10.1089/thy.2010.0429

Devries-Seimon, T., Y. Li, P.M. Yao, E. Stone, Y. Wang, R.J. Davis, R. Flavell, and I. Tabas. 2005. Cholesterol-induced macrophage apoptosis requires ER stress pathways and engagement of the type A scavenger receptor. *J. Cell Biol.* 171:61–73. https://doi.org/10.1083/jcb.200502078

Drechsler, M., J. Duchene, and O. Soehnlein. 2015. Chemokines control mobilization, recruitment, and fate of monocytes in atherosclerosis. *Arterioscler. Thromb. Vasc. Biol.* 35:1050–1055. https://doi.org/10.1161/ATVBAHA.114.304649

Galkina, E., A. Kadl, J. Sanders, D. Varughese, I.J. Sarembock, and K. Ley. 2006. Lymphocyte recruitment into the aortic wall before and during development of atherosclerosis is partially L-selectin dependent. *J. Exp. Med.* 203:1273–1282. https://doi.org/10.1084/jem.20052205

Goossens, P., M.N. Vergouwe, M.J. Gijbels, D.M. Curfs, J.H. van Woezik, M.A. Hoeksema, S. Xanthoulea, P.J. Leenen, R.A. Rupec, M.H. Hofker, and M. P. de Winther. 2011. Myeloid IκBα deficiency promotes atherogenesis by enhancing leukocyte recruitment to the plaques. *PLoS One.* 6:e22327. https://doi.org/10.1371/journal.pone.0022327

Gosling, J., S. Slaymaker, L. Gu, S. Tseng, C.H. Zlot, S.G. Young, B.J. Rollins, and I.F. Charo. 1999. MCP-1 deficiency reduces susceptibility to atherosclerosis in mice that overexpress human apolipoprotein B. *J. Clin. Invest.* 103:773–778. https://doi.org/10.1172/JCI5624

Hak, A.E., H.A. Pols, T.J. Visser, H.A. Drexhage, A. Hofman, and J.C. Witteman. 2000. Subclinical hypothyroidism is an independent risk factor for atherosclerosis and myocardial infarction in elderly women: the Rotterdam Study. *Ann. Intern. Med.* 132:270–278. https://doi.org/10.7326/0003-4819-132-4-200002150-00004

Hase, H., T. Ando, L. Eldeiry, A. Brebene, Y. Peng, L. Liu, H. Amano, T.F. Davies, L. Sun, M. Zaidi, and E. Abe. 2006. TNFalpha mediates the skeletal effects of thyroid-stimulating hormone. *Proc. Natl. Acad. Sci. USA.* 103:12849–12854. https://doi.org/10.1073/pnas.0600427103

Ivashkiv, L.B. 2011. Inflammatory signaling in macrophages: transitions from acute to tolerant and alternative activation states. *Eur. J. Immunol.* 41: 2477–2481. https://doi.org/10.1002/eji.201141783

Ivashkiv, L.B., and S.H. Park. 2016. Epigenetic Regulation of Myeloid Cells. *Microbiol. Spectr.* 4.

Johnson, J.L., and A.C. Newby. 2009. Macrophage heterogeneity in atherosclerotic plaques. *Curr. Opin. Lipidol.* 20:370–378. https://doi.org/10.1097/MOL.0b013e3283309848

Jones, R.J., L. Cohen, and H. Corbus. 1955. The serum lipid pattern in hyperthyroidism, hypothyroidism and coronary atherosclerosis. *Am. J. Med.* 19:71–77. https://doi.org/10.1016/0002-9343(55)90275-8

Kanters, E., M. Pasparakis, M.J. Gijbels, M.N. Vergouwe, I. Partouns-Hendriks, R.J. Fijneman, B.E. Clausen, I. Förster, M.M. Kockx, K. Rajewsky, et al. 2003. Inhibition of NF-kappaB activation in macrophages increases atherosclerosis in LDL receptor-deficient mice. *J. Clin. Invest.* 112:1176–1185. https://doi.org/10.1172/JCI200318580

Kanters, E., M.J. Gijbels, I. van der Made, M.N. Vergouwe, P. Heeringa, G. Kraal, M.H. Hofker, and M.P. de Winther. 2004. Hematopoietic NF-kappaB1 deficiency results in small atherosclerotic lesions with an inflammatory phenotype. *Blood.* 103:934–940. https://doi.org/10.1182/blood-2003-05-1450

Kim, H.S., S.L. Ullevig, D. Zamora, C.F. Lee, and R. Asmis. 2012. Redox regulation of MAPK phosphatase 1 controls monocyte migration and macrophage recruitment. *Proc. Natl. Acad. Sci. USA.* 109:E2803–E2812. https://doi.org/10.1073/pnas.1212596109

Kiss, E., C. Balázs, L. Bene, S. Damjanovich, and J. Matkó. 1997. Effect of TSH and anti-TSH receptor antibodies on the plasma membrane potential of polymorphonuclear granulocytes. *Immunol. Lett.* 55:173–177. https://doi.org/10.1016/S0165-2478(97)02704-1

Klein, J.R. 2003. Physiological relevance of thyroid stimulating hormone and thyroid stimulating hormone receptor in tissues other than the thyroid. *Autoimmunity.* 36:417–421. https://doi.org/10.1080/08916930310001603019

Kruger, T.E., and J.E. Blalock. 1986. Cellular requirements for thyrotropin enhancement of in vitro antibody production. *J. Immunol.* 137:197–200.

Lhoták, Š., G. Gyulay, J.C. Cutz, A. Al-Hashimi, B.L. Trigatti, C.D. Richards, S. A. Igdoura, G.R. Steinberg, J. Bramson, K. Ask, and R.C. Austin. 2016. Characterization of Proliferating Lesion-Resident Cells During All Stages of Atherosclerotic Growth. *J. Am. Heart Assoc.* 5:e003945. https://doi.org/10.1161/JAHA.116.003945

Liu, P., Y. Ji, T. Yuen, E. Rendina-Ruedy, V.E. DeMambro, S. Dhawan, W. Abu-Amer, S. Izadmehr, B. Zhou, A.C. Shin, et al. 2017. Blocking FSH induces thermogenic adipose tissue and reduces body fat. *Nature.* 546:107–112. https://doi.org/10.1038/nature22342

Lorenz, M.W., H.S. Markus, M.L. Bots, M. Rosvall, and M. Sitzer. 2007. Prediction of clinical cardiovascular events with carotid intima-media thickness: a systematic review and meta-analysis. *Circulation.* 115: 459–467. https://doi.org/10.1161/CIRCULATIONAHA.106.628875

Lou, Y., S. Liu, C. Zhang, G. Zhang, J. Li, M. Ni, G. An, M. Dong, X. Liu, F. Zhu, et al. 2013. Enhanced atherosclerosis in TIPE2-deficient mice is associated with increased macrophage responses to oxidized low-density lipoprotein. *J. Immunol.* 191:4849–4857. https://doi.org/10.4049/jimmunol.1300053

Lu, M., C.B. Yang, L. Gao, and J.J. Zhao. 2015. Mechanism of subclinical hypothyroidism accelerating endothelial dysfunction (Review). *Exp. Ther. Med.* 9:3–10. https://doi.org/10.3892/etm.2014.2037

Ma, S., F. Jing, C. Xu, L. Zhou, Y. Song, C. Yu, D. Jiang, L. Gao, Y. Li, Q. Guan, and J. Zhao. 2015. Thyrotropin and obesity: increased adipose triglyceride content through glycerol-3-phosphate acyltransferase 3. *Sci. Rep.* 5:7633. https://doi.org/10.1038/srep07633

Marians, R.C., L. Ng, H.C. Blair, P. Unger, P.N. Graves, and T.F. Davies. 2002. Defining thyrotropin-dependent and -independent steps of thyroid hormone synthesis by using thyrotropin receptor-null mice. *Proc. Natl. Acad. Sci. USA.* 99:15776–15781. https://doi.org/10.1073/pnas.242322099

Marino, F., L. Guasti, M. Cosentino, D. De Piazza, C. Simoni, V. Bianchi, E. Piantanida, F. Saporiti, M.G. Cimpanelli, C. Crespi, et al. 2006. Thyroid hormone and thyrotropin regulate intracellular free calcium concentrations in human polymorphonuclear leukocytes: in vivo and in vitro studies. *Int. J. Immunopathol. Pharmacol.* 19:149–160. https://doi.org/10.1177/205873920601900115

Medzhitov, R., and T. Horng. 2009. Transcriptional control of the inflammatory response. *Nat. Rev. Immunol.* 9:692–703. https://doi.org/10.1038/nri2634

Monzani, F., N. Caraccio, M. Kozàkowà, A. Dardano, F. Vittone, A. Virdis, S. Taddei, C. Palombo, and E. Ferrannini. 2004. Effect of levothyroxine replacement on lipid profile and intima-media thickness in subclinical hypothyroidism: a double-blind, placebo- controlled study. *J. Clin. Endocrinol. Metab.* 89:2099–2106. https://doi.org/10.1210/jc.2003-031669

Moore, J.P., S. Sakkal, M.L. Bullen, B.K. Kemp-Harper, S.D. Ricardo, C.G. Sobey, and G.R. Drummond. 2013. A flow cytometric method for the analysis of macrophages in the vascular wall. *J. Immunol. Methods.* 396: 33–43. https://doi.org/10.1016/j.jim.2013.07.009

Park, S.H., Y. Sui, F. Gizard, J. Xu, J. Rios-Pilier, R.N. Helsley, S.S. Han, and C. Zhou. 2012. Myeloid-specific IκB kinase β deficiency decreases atherosclerosis in low-density lipoprotein receptor-deficient mice. *Arterioscler. Thromb. Vasc. Biol.* 32:2869–2876. https://doi.org/10.1161/ATVBAHA.112.254573

Potteaux, S., E.L. Gautier, S.B. Hutchison, N. van Rooijen, D.J. Rader, M.J. Thomas, M.G. Sorci-Thomas, and G.J. Randolph. 2011. Suppressed monocyte recruitment drives macrophage removal from atherosclerotic plaques of Apoe-/- mice during disease regression. *J. Clin. Invest.* 121:2025–2036. https://doi.org/10.1172/JCI43802

Randolph, G.J. 2014. Mechanisms that regulate macrophage burden in atherosclerosis. *Circ. Res.* 114:1757–1771. https://doi.org/10.1161/CIRCRESAHA.114.301174

Ricci, R., G. Sumara, I. Sumara, I. Rozenberg, M. Kurrer, A. Akhmedov, M. Hersberger, U. Eriksson, F.R. Eberli, B. Becher, et al. 2004. Requirement of JNK2 for scavenger receptor A-mediated foam cell formation in atherogenesis. *Science.* 306:1558–1561. https://doi.org/10.1126/science.1101909

Rivera-Torres, J. 2015. Analysis of Gene and Protein Expression in Atherosclerotic Mouse Aorta by Western Blot and Quantitative Real-Time PCR. *Methods Mol. Biol.* 1339:309–322. https://doi.org/10.1007/978-1-4939-2929-0_21

Robbins, C.S., I. Hilgendorf, G.F. Weber, I. Theurl, Y. Iwamoto, J.L. Figueiredo, R. Gorbatov, G.K. Sukhova, L.M. Gerhardt, D. Smyth, et al. 2013. Local proliferation dominates lesional macrophage accumulation in atherosclerosis. *Nat. Med.* 19:1166–1172. https://doi.org/10.1038/nm.3258

Rodondi, N., W.P. den Elzen, D.C. Bauer, A.R. Cappola, S. Razvi, J.P. Walsh, B. O. Asvold, G. Iervasi, M. Imaizumi, T.H. Collet, et al.; Thyroid Studies Collaboration. 2010. Subclinical hypothyroidism and the risk of coronary heart disease and mortality. *JAMA.* 304:1365–1374. https://doi.org/10.1001/jama.2010.1361

Saederup, N., L. Chan, S.A. Lira, and I.F. Charo. 2008. Fractalkine deficiency markedly reduces macrophage accumulation and atherosclerotic lesion formation in CCR2-/- mice: evidence for independent chemokine functions in atherogenesis. *Circulation.* 117:1642–1648. https://doi.org/10.1161/CIRCULATIONAHA.107.743872

Sather, S., K.D. Kenyon, J.B. Lefkowitz, X. Liang, B.C. Varnum, P.M. Henson, and D.K. Graham. 2007. A soluble form of the Mer receptor tyrosine kinase inhibits macrophage clearance of apoptotic cells and platelet aggregation. *Blood.* 109:1026–1033. https://doi.org/10.1182/blood-2006-05-021634

Schneider, J.G., B.N. Finck, J. Ren, K.N. Standley, M. Takagi, K.H. Maclean, C. Bernal-Mizrachi, A.J. Muslin, M.B. Kastan, and C.F. Semenkovich. 2006. ATM-dependent suppression of stress signaling reduces vascular disease in metabolic syndrome. *Cell Metab.* 4:377–389. https://doi.org/10.1016/j.cmet.2006.10.002

Sellitti, D.F., D. Dennison, T. Akamizu, S.Q. Doi, L.D. Kohn, and H. Koshiyama. 2000. Thyrotropin regulation of cyclic adenosine monophosphate production in human coronary artery smooth muscle cells. *Thyroid*. 10: 219–225. https://doi.org/10.1089/thy.2000.10.219

Shahrara, S., S.R. Pickens, A.M. Mandelin II, W.J. Karpus, Q. Huang, J.K. Kolls, and R.M. Pope. 2010. IL-17-mediated monocyte migration occurs partially through CC chemokine ligand 2/monocyte chemoattractant protein-1 induction. *J. Immunol.* 184:4479–4487. https://doi.org/10.4049/jimmunol.0901942

Shibata, N., and C.K. Glass. 2009. Regulation of macrophage function in inflammation and atherosclerosis. *J. Lipid Res.* 50(Suppl):S277–S281. https://doi.org/10.1194/jlr.R800063-JLR200

Song, Y., C. Xu, S. Shao, J. Liu, W. Xing, J. Xu, C. Qin, C. Li, B. Hu, S. Yi, et al. 2015. Thyroid-stimulating hormone regulates hepatic bile acid homeostasis via SREBP-2/HNF-4α/CYP7A1 axis. *J. Hepatol.* 62:1171–1179. https://doi.org/10.1016/j.jhep.2014.12.006

Swirski, F.K., and M. Nahrendorf. 2013. Leukocyte behavior in atherosclerosis, myocardial infarction, and heart failure. *Science*. 339:161–166. https://doi.org/10.1126/science.1230719

Takeuch, O., and S. Akira. 2011. Epigenetic control of macrophage polarization. *Eur. J. Immunol.* 41:2490–2493. https://doi.org/10.1002/eji.201141792

Tian, L., Y. Song, M. Xing, W. Zhang, G. Ning, X. Li, C. Yu, C. Qin, J. Liu, X. Tian, et al. 2010. A novel role for thyroid-stimulating hormone: up-regulation of hepatic 3-hydroxy-3-methyl-glutaryl-coenzyme A reductase expression through the cyclic adenosine monophosphate/protein kinase A/cyclic adenosine monophosphate-responsive element binding protein pathway. *Hepatology*. 52:1401–1409. https://doi.org/10.1002/hep.23800

Touboul, P.J., M.G. Hennerici, S. Meairs, H. Adams, P. Amarenco, N. Bornstein, L. Csiba, M. Desvarieux, S. Ebrahim, R. Hernandez Hernandez, et al. 2012. Mannheim carotid intima-media thickness and plaque consensus (2004-2006-2011). An update on behalf of the advisory board of the 3rd, 4th and 5th watching the risk symposia, at the 13th, 15th and 20th European Stroke Conferences, Mannheim, Germany, 2004, Brussels, Belgium, 2006, and Hamburg, Germany, 2011. *Cerebrovasc. Dis.* 34:290–296. https://doi.org/10.1159/000343145

Wang, J., M. Whetsell, and J.R. Klein. 1997. Local hormone networks and intestinal T cell homeostasis. *Science*. 275:1937–1939. https://doi.org/10.1126/science.275.5308.1937

Zhao, M., L. Liu, F. Wang, Z. Yuan, X. Zhang, C. Xu, Y. Song, Q. Guan, L. Gao, Z. Shan, et al. 2016. A Worthy Finding: Decrease in Total Cholesterol and Low-Density Lipoprotein Cholesterol in Treated Mild Subclinical Hypothyroidism. *Thyroid*. 26:1019–1029. https://doi.org/10.1089/thy.2016.0010